Proc Soc Antiq Scot 142 (2012), 63–132

Croig Cave: a Late Bronze Age ornament deposit and three millennia of fishing and foraging on the north-west coast of Mull, Scotland

Steven Mithen* and Karen Wicks†
with contributions from Phil Austin, Stuart Black, Trevor Cowie, Sarah Elliott, Claire Ingrem, Brendan O'Connor and Sam Smith

ABSTRACT

Activity within caves provides an important element of the later prehistoric and historic settlement pattern of western Scotland. This contribution reports on a small-scale excavation within Croig Cave, on the coast of north-west Mull, that exposed a 1.95m sequence of midden deposits and cave floors that dated between c *1700* BC *and* AD *1400. Midden analysis indicated the processing of a diverse range of small fish and the collection of shellfish throughout this period, showing a high degree of continuity involving low-risk, inshore fishing. At* c *950* BC*, a penannular copper bracelet and an amber bead were deposited within a small, shallow pit within the cave floor, suggestive of a discrete ritual episode within the cycle of otherwise potentially mundane activities. Lead isotope analysis indicates an Irish origin for the copper ore. A piece of iron slag within later midden deposits, dated to* c *400* BC*, along with high frequencies of wood charcoal, suggest that smithing or smelting may have occurred within the cave. High zinc levels in the historic levels of the midden* c AD *1200 might indicate intensive processing of seaweed.*

INTRODUCTION

Croig Cave is located in a low cliff, above a steep slope made of large basalt boulders, facing south across Croig Bay, Isle of Mull (NGR:NM 38595442, illus 1). It is a small cave, with a maximum height of *c* 2.5m at the front, a maximum width of *c* 5m and length of *c* 8m (illus 2). The current cave floor is 6.1m above the present-day high tide mark, with the collapsed boulders forming a bank approximately two metres high, in front of the cave mouth. Our attention was drawn to Croig Cave by a local resident (Ian Spence) during the course of a survey in north-west Mull for Mesolithic and early Neolithic settlement as part of the Inner Hebrides Mesolithic Project. Although its topographic position was not especially promising for Mesolithic archaeology, a trial trench was excavated to explore its deposits.

Initial work in August 2006 exposed 1.20m depth of shell-midden; a piece of wood charcoal at 1.03m depth returned an AMS date of 2639 ± 50 BP (Beta-221404). Further excavation in August 2007 reached the base of the cave at a depth of 1.90m and recovered three artefacts: a piece of iron-working slag, an

* Vice-Chancellor's Office, Whiteknights House, University of Reading, Reading RG6 6AH
† Department of Archaeology, University of Reading, PO Box 227, Reading RG6 6AB

ILLUS 1 View of Croig Cave within the basalt cliff of northwest Mull, looking north towards the Isle of Rùm in the distance

amber bead and a copper bracelet. The slag came from within the shell midden itself, while the bracelet and bead came from a pit dug into an earthen floor at a depth of 1.20m. As such, Croig Cave provided an opportunity to place these artefacts into their archaeological context by an analysis of their associated deposits and to explore long-term coastal foraging from the later prehistoric to historic periods on the west coast of Scotland. A variety of analytical methods were used to characterise the sediments and midden deposits with the aim of reconstructing past human activity and site formation processes.

DATA RECOVERY

EXCAVATION

with Sam Smith

Prior to excavation, more than half of the cave floor was covered by large boulders and rocks from roof and wall collapse, between which limpet (*Patella* sp) and periwinkle (*Littorina* sp) shells were exposed. A 1m^2 test-trench was excavated in the frontal area of the cave (illus 2; illus 3), approximately 2m from the current drip line and close to the western wall. When the depth of deposits reached 150cm, a

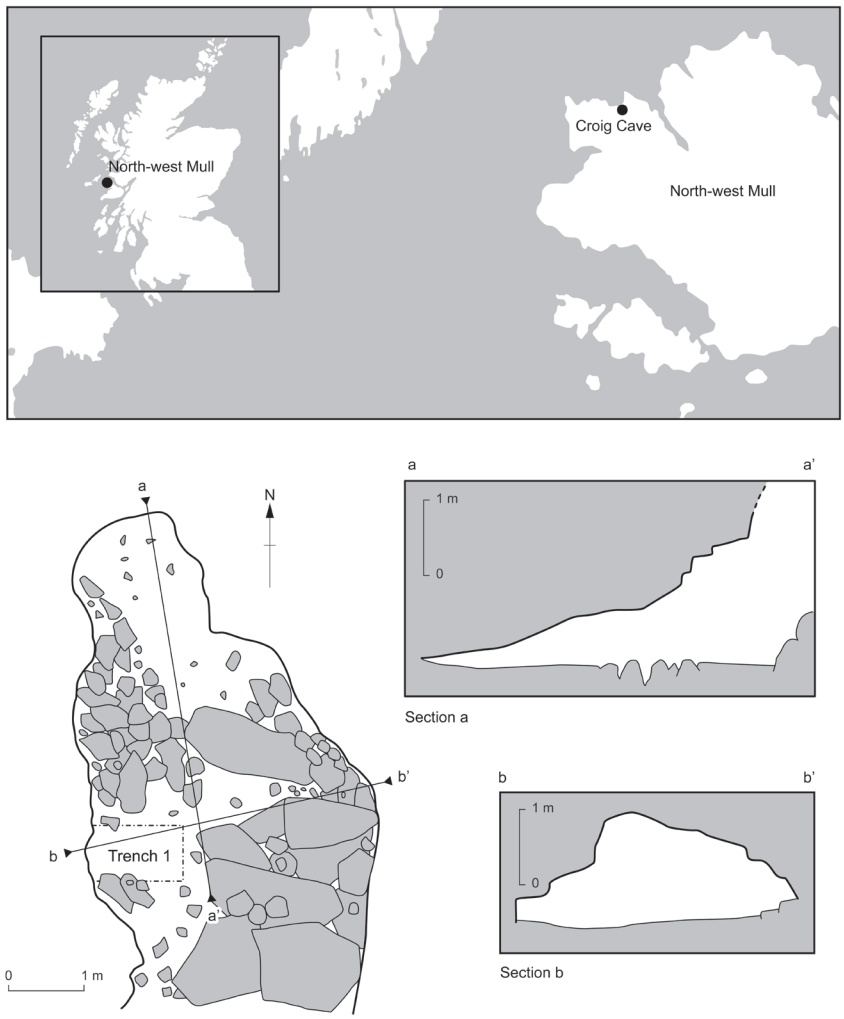

ILLUS 2 Location, plan and profiles of Croig Cave, showing location of excavation trench

step was excavated on the southern side of the trench to enable access to the deeper deposits and the trench was extended to the western wall of the cave. Excavation continued to a depth of 190cm, at which bedrock was reached.

The excavation was undertaken stratigraphically, based on in-field observations of variations in sediment characteristics (illus 4, 5 and 6; Table 1). Sixteen 5-litre bulk samples of sediment were taken at approximately 10cm intervals through the depth of deposits (Samples CCBS:1 to CCBS:16) and these provided material for the sedimentary and midden analysis described below. Large bone fragments were hand-picked from the deposits during excavation.

A single sample of unidentified wood charcoal (CCRS:1), coming from a depth of 103cm, was submitted for AMS dating, at the end of the initial excavation in 2006. This was to evaluate the approximate date of the deposit because no artefacts or other

ILLUS 3 Excavation within Croig Cave, August 2007

indications of its period of formation had been recovered. This returned a date of 2639 ± 50 BP (Beta-221404) (Table 2). In light of that date, excavation continued in 2007 and a dating programme, based on limpet shells, was implemented to establish the chronology of the midden deposit. Limpet shells were chosen because the same specimens could also provide palaeoenvironmental information via oxygen isotope analysis.

Individual shells for AMS radiocarbon dating were hand-picked, either directly from the shell-midden section at levels corresponding to the bulk samples or from material within the five-litre bulk samples. These shells were further inspected in the laboratory for their quality of preservation and risk of contamination by examining surface characteristics such as the presence of residues, pitting, erosion and fracture; any shells that had such characteristics were rejected. This resulted in 13 being selected for AMS dating, coming from 10cm to 25cm intervals throughout the depth of the deposit (CCRS:2 to CCRS:14). Each of the selected shells was cut in half, with one portion submitted to Beta-Analytic and the other utilised for oxygen isotope analysis to reconstruct sea surface temperatures, the results of which have been reported elsewhere (Wang et al 2012).

STRATIGRAPHIC SEQUENCE

Below the rubble of the cave floor there was *c* 25cm of silty-sand with angular rocks and occasional shell and bone (Context CC101). This horizon contained a thin layer of yellowish clay at its southern extent, with such lenses being frequent throughout the sequence. Below CC101, there was a thin layer of reddish sandy-silt, with shell and angular rocks (Context CC102a). This was slightly thicker to the south and west, a common feature of the stratigraphy. It was followed by a thick layer of dense shell-midden deposit within a black silty matrix (Context CC102b) (illus 3 and 4) with lenses of

ash, charcoal and yellowish clay. These lenses were patchy and impossible to follow in plan within the small confines of the trench and the cramped conditions of the cave, with some evident in the trench section (illus 5). The base of CC102b varied between 90cm and 75cm below the modern ground surface, the deposit sloping towards the south.

The dense midden deposit continued, but with a change in the matrix to a reddish silty-sand with charcoal-rich lenses and a thin horizon of yellowish silty-sand towards its base, varying between 1cm in the south to 5cm in the north (Context CC103a). This was above a *c* 10cm thick horizon with similar characteristics, but with a change in the matrix

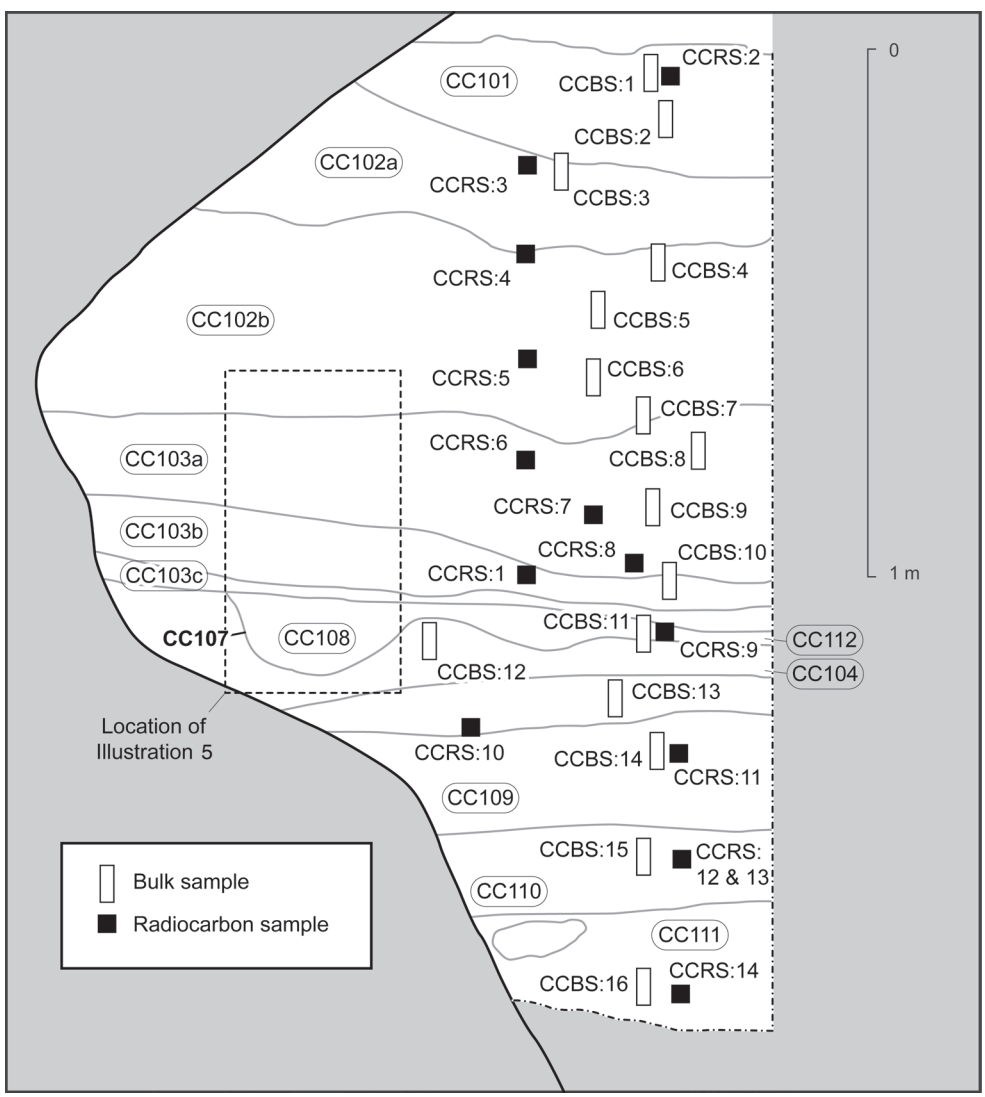

ILLUS 4 Schematic south-facing section of Trench 1, Croig Cave, showing stratigraphic units and location of bulks samples (CCBS:1-16) and dating samples (CCRS:1-14)

Table 1
Contexts, bulk samples and radiocarbon dating samples

Context (depth, m)	*Description*	*Bulk samples (depth, m) / air dry weight, g*	*Dating sample (depth, m)*
CC101 (0.00–0.25)	Dark brown silty sand with large angular autochthonous basalt clasts (roof collapse), with occasional bone and shell. Above CC102a.	CCBS:1 (0.02–0.10) / 3843.9 CCBS:2 (0.12–0.20) / 2267.0	CCRS:2 (0.06)
CC102a (0.25–0.40)	Reddish-brown silty sand with angular basalt clasts, Frequent shell and bone, often in patchy lenses. Below CC101, above CC102b.	CCBS:3 (0.22–0.30) / 7102.5	CCRS:3 (0.23)
CC102b (0.40–0.70)	Black silt with occasional clasts and cobbles, some of which are burnt. Abundant (>90%) shell and bone fragments. Contains lenses of ash, charcoal and burnt clay. Becomes more reddish-brown towards base of context. Below CC102a, above CC103a.	CCBS:4 (0.39–0.47) / 5106.7 CCBS:5 (0.47–0.55) / 4499.0 CCBS:6 (0.60–0.68) / 3535.4 CCBS:7 (0.67–0.75) / 4235.4	CCRS:4 (0.42) CCRS:5 (0.61)
CC103a (0.70–1.0)	Dark reddish brown sandy silt with lenses of shells, ash and charcoal. A lens of pale sandy silt towards its base, which is 5cm thick at southern edge and thins to 0.5cm at northern edge. Below CC102b, above CC103b.	CCBS:8 (0.76–0.84) / 4756.7 CCBS:9 (0.84–0.92) / 5419.1	CCRS:6 (0.82) CCRS:7 (0.92) CCRS: 8 (1.02)
CC103b (1.0–1.10)	Pale reddish-brown sandy silt, with high frequency of shells, ash and charcoal lenses towards the base. Below CC103a, above CC103c.	CCBS:10 (0.97–1.05) / 6734.7	CCRS:1 (1.03)
CC103c (1/15–1.20)	Thin layer of light, greyish-brown sandy silt. Below CC103b, above CC104, CC108 and CC112.		
CC112 (1.10–1.15)	Thin layer of dark reddish-brown midden material, similar to CC106 and CC108. Below CC103c, above CC104.	CCBS:11 (1.08–1.19) / 4766.2	CCRS: 9 (1.14)
CC104 (1.15–1.20)	Compact greenish sandy clay, with charcoal flecks, occasional shell and lenses of more reddish sediment. The context is thicker towards the west side of the trench. Below CC103c and CC108, above CC109.	CCBS:12 (1.12–1.20) / 6076.9	
CC105 (1.15)	Sub-circular cut for shallow pit, irregular in plan and profile, with diameter 0.33m. Only partially excavated because it extended below south facing section. Cuts CC104, contains pit fill CC106.		

Context (depth, m)	*Description*	*Bulk samples (depth, m) / air dry weight, g*	*Dating sample (depth, m)*
CC107 (1.15)	Sub-circular cut for a shallow pit, irregular in both profile and plan, with diameter of 0.27m. Only partially excavated because it extended below the north facing section. Cuts CC107, contains pit fill CC108.		
CC108	Dark, reddish-brown, charcoal rich fill of Cut CC107 containing shell, bracelet and bead. Below CC103c, above CC104.		
CC109 (1.20–1.50)	Reddish-brown sandy silt, with occasional shell, bone and charcoal, becoming thicker towards the west. Below CC104, above CC110.	CCBS:13 (1.22–1.30) / 7511.2 CCBS:14 (1.33–1.41) / 6622.9	CCRS:10 (1.33) CCRS:11 (1.35)
CC110 (1.50–1.65)	Greenish, grey silty sand, with occasional shell, bone and charcoal. Below CC109, above CC111 and bedrock.	CCBS:15 (1.52–1.60) / 6173.8	CCRS:12 (1.55) CCRS:13 (1.56)
CC111 (1.65–1.90)	Reddish-brown sandy silty sand, with occasional shell, bone and charcoal. Only exposed in the east of the trench. Below CC110, above bedrock.	CCBS:16 (1.78–1.86) / 5359.1	CCRS:14 (1.81)

to a pale brown sandy-silt (Context CC103b) A piece of iron slag was recovered at a depth of 110cm. Underlying this context there was a *c* 5cm layer of light greyish-brown sandy silt (Context CC103c) with significantly fewer shells and charcoal fragments (illus 5).

At the base of CC103c, 115cm below the modern day surface, the deposits in the cave changed their nature to become consolidated horizons with the character of trampled floors rather than midden accumulations. Context CC112 was a *c* 5cm thick reddish-brown horizon that began 30cm east of the west wall of the cave. Removal of this exposed a compact layer of green sandy clay (Context CC104) that covered the entire surface of the trench and contained two sub-circular pits, both partially covered by the trench sections (illus 7). The most northerly (Cut CC107, Fill CC108), with a diameter of *c* 27cm, was partially concealed by the south-facing section; the southerly pit (Cut CC105, Fill CC106) was of similar size (diameter *c* 33cm) but more irregular. CC107 and CC105 were shown to be shallow, being more accurately described as scoops or depressions rather than pits. The fills (CC108, CC106) were effectively identical dark brown silty-sand with charcoal inclusions, and similar to Context CC112 with which they appeared continuous. These three contexts (CC108, CC106 and CC112) may indeed have been one single horizon which filled depressions within the underlying surface (CC104). CC108, the fill of scoop CC107 contained a bracelet and an amber bead (illus 8).

Below CC104, at 120cm, there was a *c* 30cm thick layer of compacted reddish silty-sand, with some shell, bone and charcoal fragments (Context CC109). This covered the entire trench, with bedrock now becoming exposed as the western wall of the cave was sloping steeply to the east. Elsewhere, CC109 was above Context CC110, which had similar characteristics but more greenish in colour and extended to a depth of 165cm, with increasing

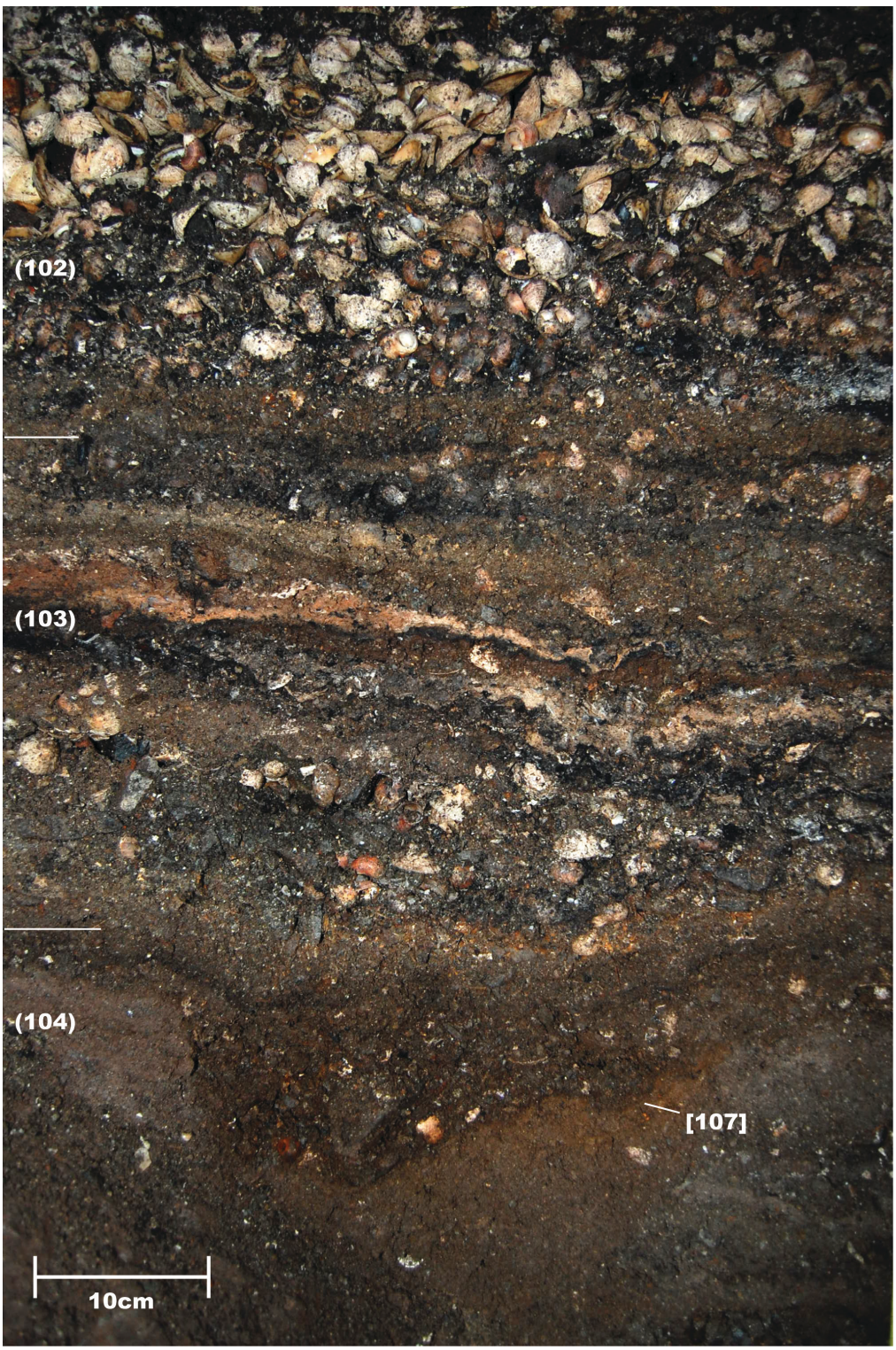

ILLUS 5 South-facing section, Croig Cave

TABLE 2
Radiocarbon determinations and their calibrations

Sample no	*Laboratory code*	*Material*	$\delta^{13}C$ (‰)	*Radiocarbon Age (^{14}C years BP)*	*Cal BP (68.2% probability)*	*Cal BP (95.4% probability)*	*Cal BC (68.2% probability)*	*Cal BC (95.4% probability)*
CCRS:2	Beta-251116	Shell	–0.2	1070 ± 40	750–630	820–550	AD 1200–1320	AD 1130–1400
CCRS:3	Beta-252891	Shell	+0.5	1160 ± 40	840–690	900–660	AD 1110–1260	AD 1050–1290
CCRS:4	Beta-252892	Shell	+0.2	2340 ± 40	2120–1950	2140–1870	170–1	290–80
CCRS:5	Beta-251117	Shell	+0.7	2510 ± 40	2320–2160	2400–2070	370–210	450–120
CCRS:6	Beta-252894	Shell	+0.7	2450 ± 40	2280–2110	2330–2010	340–160	380–60
CCRS:7	Beta-251118	Shell	–0.1	2360 ± 40	2150–1970	2270–1900	200–20	320–50
CCRS:8	Beta-252893	Shell	+1.3	2510 ± 40	2320–2160	2400–2070	370–210	450–120
CCRS:1	Beta-221404	Charcoal	–26.4	2630 ± 50	2790–2710	2860–2540	850–770	920–590
CCRS:9	Beta-251121	Shell	+1.0	3030 ± 40	2940–2780	3040–2730	1000–830	1090–780
CCRS:10	Beta-252895	Shell	+0.8	3330 ± 40	3350–3190	3410–3070	1400–1240	1460–1130
CCRS:11	Beta-251119	Shell	+1.0	3390 ± 40	3410–3250	3480–3160	1460–1300	1530–1210
CCRS:12	Beta-252897	Shell	+1.5	3370 ± 40	3390–3230	3460–3140	1440–1280	1510–1190
CCRS:13	Beta-252896	Shell	+0.9	3520 ± 40	3560–3400	3630–3330	1610–1450	1690–1390
CCRS: 14	Beta-251120	Shell	+0.5	2420 ± 40	2250–2060	2310–1980	310–110	360–30

ILLUS 6 Detail of south-facing section Croig Cave, showing pit CC107 and the many small lenses within contexts CC103a–c, discontinuous in plan

amounts of bedrock exposed. The final deposits (CC111) were only present in the eastern half of the trench and difficult to access within the cramped conditions of the cave and the narrow dimensions of the trench. CC111 was similar to CC110, but with basalt fragments and a higher frequency of gravel in the matrix. Excavation of this deposit was halted at a depth of 185cm when bedrock covered *c* 90% of the base of the trench, with the estimation that entire bedrock would be reached at 190cm.

LABORATORY METHODS

The 16 bulk samples were air-dried, weighed and split into two representative sub-samples. Each of the first set of sub-samples was separated into its 4mm, 2mm, 1mm and 500µm fractions by wet-sieving. The dried residues were sorted for archaeological material, which fell into three categories: shell, bone and wood charcoal. This material was retrieved from the sedimentary matrix by hand sorting, assisted by the use of a Leica S6 stereo-binocular microscope at ×10–60 magnifications. There was a complete absence of artefactual material within the bulk samples. The second set of 16 sub-samples provided sediments for physical and geochemical analysis, with the <2.0mm fraction being used to identify bulk mineralogy and elemental composition.

To assist in the sedimentary analysis, two control sediment samples were collected from the vicinity of the Croig Cave midden. Spot samples of cave earth from the modern floor surface were taken at various locations within

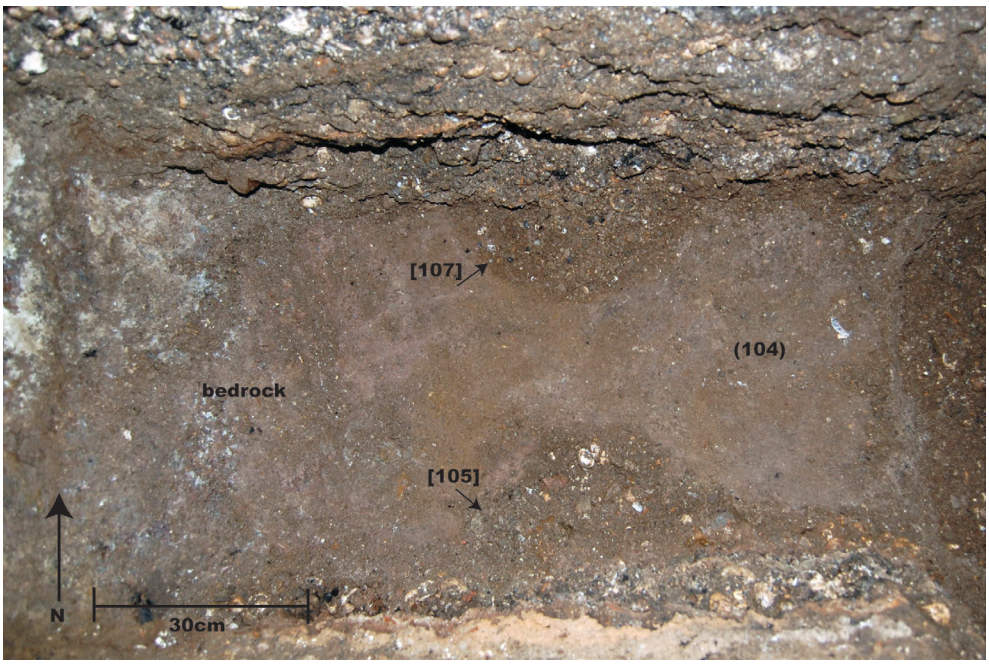

ILLUS 7 Context CC104 from above, showing bedrock of the western wall of the cave (left) and the two pits, CC107 and CC105, partially covered by the south and north facing sections respectively

ILLUS 8 The bracelet in situ within fill CC108 of pit CC107, from above

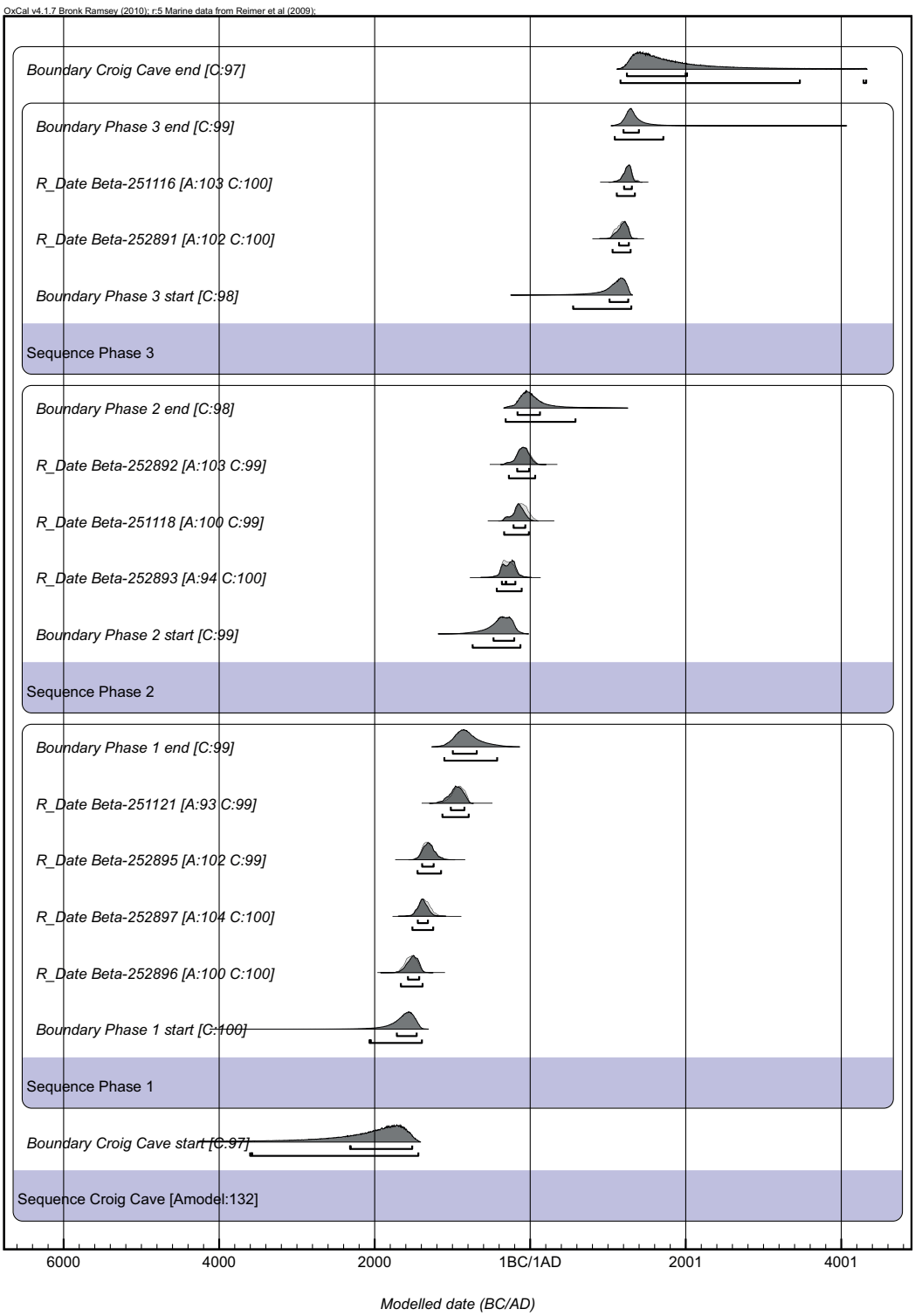

ILLUS 9 Posterior probability distributions of dates from Croig Cave showing 68.2% and 95.4% highest posterior density regions. The model is constrained overall by the sequence boundary (large rectangle with rounded corners) and the phase boundaries (small rectangles with rounded corners), along with the OxCal keyword

the cave, but away from the midden, to provide an ostensibly autochthonous control sample (Control 1, CCBS:17). Then, a bulk sample of beach sand was collected from various locations on the foreshore and backshore at Croig, to provide an allochthonous control sample (Control 2, Sample CCBS:18).

Radiocarbon measurements and calibrations for the 13 shell samples (CCRS:2 to CCRS:14) and one piece of wood charcoal (CCRS:1) were provided by Beta-Analytic. From these, the chronology of human activity within Croig Cave was established via Bayesian modelling, using methods described within Appendix 1. That appendix also describes the background and methods for the lead isotope analysis of the slag and bracelet and the analytical methods for sediment characterisation using X-ray diffraction (XRD), X-ray fluorescence (XRF), particle size distribution (PSD), loss on ignition (LOI), and magnetic susceptibility. In addition, Appendix 1 provides the analytical methods used in the classification and interpretation of the shell, bone and wood charcoal recovered from the sieve residues.

RADIOCARBON DATING, BAYESIAN MODELLING AND PHASING

The calibrated results for the 14 AMS dated samples from Croig Cave are given in Table 2. These were used to construct a Bayesian chronological model for the shell midden, which has acceptable agreement indices (ie in excess of 60%; Amodel 131.8%; Aoverall 99.8%) and convergence values (> 95%) (illus 9). Furthermore, all $\delta^{13}C$ values obtained for the shell and wood charcoal samples are in accordance with those expected for marine carbonates and C3 plants respectively (Walker 2005: 26), demonstrating the integrity of the radiocarbon samples. This analysis indicates that activity linked to the formation of the midden spanned three millennia, with three phases of intense activity.

PHASE 1

This phase comprises the lower stratigraphic units incorporating contexts CC111, CC110, CC109, CC112, CC104, CC108 and CC106, from which six AMS dates were derived (Beta-251120, Beta-252896, Beta-252897, Beta-251119, Beta-252895 and Beta-25112). Samples CCBS:11 to CCBS:16 relate to this phase of activity.

The six AMS radiocarbon dates provided a group of calibrated values falling within the late 1st to late 2nd millennium cal BC, with the exception of Beta-251120 coming from CC111 at the base of the sequence (Table 2). That provided a considerably younger date, corresponding to those obtained from Phase 2 (see below). This date was, therefore, excluded from the Bayesian model as we consider it to represent contamination from younger material that had fallen from the exposed section in Trench 1, probably during excavation. As noted above, CC111 was the deepest deposit at the base of a narrow trench through unconsolidated shell midden and hence such contamination is not surprising. Beta-251119 coming from CC109 was also eliminated because it was older than samples that were stratigraphically lower down the sequence. Such stratigraphic inversions are not unexpected within narrow trenches through shell middens because these are known to have complex formation histories with interleaving dumps of material and post-depositional mixing. Indeed, it is quite surprising that 10 of the 14 AMS dates from the small trench in Croig Cave were in 'correct' stratigraphic order.

Posterior density estimates (Table 3; illus 9) place the start of accumulation of the shell midden (base of Phase 1) between *1720–1460 cal BC* (*3670–3400 cal BP*; 68.2% probability) and *2070–1390 cal BC* (*4020–3340 cal BP*; 95.4% probability). The end of Phase 1 dates to between *1000–690 cal BC* (*2950–2630 cal BP*; 68.2% probability) and 1110–420 cal BC (3060–2370 cal BP; 95.4% probability). As such,

TABLE 3
Calibrated radiocarbon age ranges and posterior density estimates

Sample no	*Laboratory code*	*Posterior density estimate cal BC/AD (95.4% probability)*	*Posterior density estimate cal BP (95.4% probability)*
CCRS:2	Beta-251116	cal AD 1110–1360	840–590
CCRS:3	Beta-252891	cal AD 1050–1300	900–650
CCRS:4	Beta-252892	270 cal BC–cal AD 70	2220–1880
CCRS:5	Beta-251118	340–10 cal BC	2290–1960
CCRS:8	Beta-252893	440–100 cal BC	2380–2050
CCRS:9	Beta-251121	1130–790 cal BC	3080–2740
CCRS:10	Beta-252895	1450–1140 cal BC	3400–3090
CCRS:12	Beta-252897	1520–1240 cal BC	3470–3190
CCRS:13	Beta-252896	1670–1380 cal BC	3620–3330

most of Phase 1 activity can be characterised as falling within the Bronze Age.

The bracelet and amber bead were found in a pit fill (CC108) similar in composition and stratigraphically consistent with CC112, from which the shell providing date Beta-251121 was acquired. As such, the best approximation for the deposition of the bracelet and bead in the midden is provided by a posterior density estimate of Beta-251121 from CC112, placing it between 1030–840 cal BC (2980–2790 cal BP; 68.2% probability) and 1130–790 cal BC (3080–2740 cal BP; 95.4% probability).

TABLE 4
Statistically consistent radiocarbon dates

Phase	*Radiocarbon sample nos*	*Laboratory codes*	X^2
3	CCRS:2 & 3	Beta-251116 & Beta-252891	Df = 1; T = 2.5 (5% = 3.8)
2	CCRS:4, 6, 7 & 14	Beta-252892, Beta-252894, Beta-251118 & Beta-251120	Df = 3; T = 4.9 (5% = 7.8)
2	CCRS:4 & 8	Beta-251117 & Beta-252893	Df = 1; T = .1 (5% = 3.8)
1	CCRS:10, 11 & 12	Beta-252897, Beta-251119 & Beta-252895	Df = 2; T = 1.2 (5% = 6.0)

TABLE 5
Average sediment accumulation rates

Phase	*Depth (m below surface)*	*Maximum period of deposition (years; 95.4% probability)*	*Sedimentation rate (cm/year)*
3	–0.25 to 0.00	1210	0.02
2	–1.20 to –0.25	1360	0.07
1	–1.90 to –1.20	1650	0.04

Three of the radiocarbon dates (Beta-252897, Beta-251119 and Beta-252895) obtained from material contained in the lowest levels of the midden were shown to be statistically consistent (χ^2-test: Df = 2; T = 1.2; 5% = 6.0; Table 4). When considered alongside the statistically inconsistent radiocarbon dates (Beta-252896 and Beta-251121) derived from Phase 1, we identified a minimum of three depositional events resulting in the deposition of midden material during the late 1st to late 2nd millennium cal BC. The calibrations indicate that these may have been centred on *c* 1530 cal BC (*c* 3480 cal BP; 95.4% probability; Beta-252896), *c* 1340 cal BC (*c* 3290 cal BP; 95.4% probability; Beta-252897, Beta-251119 and Beta-252895) and *c* 960 cal BC (*c* 2910 cal BP; 95.4% probability; Beta-251121).

The average sedimentation rate (cm/year) was calculated to be a minimum of 0.04cm/year between *c* 2070 cal BC (95.4% probability for lower boundary) to *c* 420 cal BC (95.4% probability for upper boundary; Table 5).

PHASE 2

This phase comprises contexts CC103 and CC102b in the upper levels of the midden, from which six AMS dates were acquired (Beta-221404, Beta-252893, Beta-251118, Beta-252894, Beta-251117 and Beta-252892). As such, CCBS:4 to CCBS:10 derive from Phase 2 activity.

The six calibrated AMS dates provided a group falling within the mid- to late 1st millennium cal BC (Table 2), with the dates in stratigraphic agreement except for Beta-252894 and Beta-251117. These were removed from the chronological model, as was Beta-221404, the date derived from unidentified wood charcoal. Although it is in stratigraphic agreement with dates obtained immediately below and above its level (103cm), the unidentified nature of the sample leaves open the possibility for old wood contamination. With these samples removed from the chronological model the agreement indices reach acceptable levels.

Posterior density estimates (Table 3) place the start of the accumulation of CC103, representing the base of Phase 2 and positioned immediately above the pit complex containing the bracelet and amber bead, at between 480–200 cal BC (2430–2150 cal BP; 68.2% probability) and 750–120 cal BC (2700–2070 cal BP; 95.4% probability). The end of accumulation during Phase 2 is placed between 170 cal BC–cal AD 140 (2110–1810 cal BP; 68.2% probability) and 320 cal BC–cal AD 610 (2270–1340 cal BP; 95.4% probability). As such, Phase 2 activity can be characterised as falling within the Iron Age.

The piece of iron slag was found in CC103b, from which dating sample CCRS:1 (Beta-221404) was also recovered. That provided a calibrated value of 850–770 cal BC (2790–2710 cal BP; 68.2% probability) and 920–590 cal BC (2860–2540 cal BP; 95.4% probability), which, at face value, would imply the iron slag dated to *c* 780 cal BC. The calibrated value of Beta-221404 is, however, considerably older than other samples from this phase and may be influenced by an old wood effect, the sample being an unidentified piece of wood charcoal. Consequently, we prefer to draw on the Bayesian chronological model for estimating the age of the slag and suggest that a date of *c* 400 BC is most reasonable.

Two sets of radiocarbon dates obtained from material collected from Phase 2 were shown to be statistically consistent (Table 4): Beta-252893 and Beta-251117 which were identical; Beta-251118, Beta-252894 and Beta-252892 formed the other set. Furthermore, Beta-251120, the anomalous date within Phase 1, proved to be statistically consistent with one of these sets in Phase 2 (χ^2-test: Df = 3, T = 4.9, 5%=7.8). This substantiates the suggestion that it had derived from material dislodged from the upper levels of the section face during excavation. The statistical consistency of radiocarbon dates indicates that a minimum of two depositional events resulted in the accumulation of midden during Phase 2, with the calibrations indicating that these may have been centred on 290 cal BC (*c* 2240 cal BP; 95.4% probability; Beta-252893 and Beta-251117) and *c* 190 cal BC (*c* 2110 cal BP; 95.4% probability; Beta-251118, Beta-252894, Beta-252892 and Beta-251120). If the wood charcoal date (Beta-221404) is taken at face value then a further deposition event is possible, centred on *c* 780 cal BC (*c* 2700 cal BP; 95.4% probability; Beta-221404). As noted above, we suspect that

ILLUS 10 Lump of run slag from Croig Cave Context CC103b

the chronological discrepancy suggests that this sample is influenced by an old wood effect.

The average sedimentation rate was calculated to be a minimum of 0.07cm/year between *c* 750 cal BC (*c* 2700 cal BP; 95.4% probability) and *c* cal AD 610 (*c* 1340 cal BP; 95.4% probability; Table 5).

PHASE 3

This phase comprises contexts CC102a and CC101and has two AMS dates (Beta-252891 and Beta-251116). Samples CCBS:1 to CCBS:3 relate to this final phase of activity. The two radiocarbon dates were in stratigraphic agreement and fell within the early centuries of the 2nd millennium cal AD (Table 2). Posterior density estimates (Table 3) placed the start of this Phase 3 accumulation of shell midden at between cal AD 1010–1260 (940–690 cal BP; 68.2% probability) and cal AD 530–1300 (1420–650 cal BP; 95.4% probability); the end of Phase 3 is placed at between cal AD 1200–1410 (750–540 cal BP; 68.2% probability) and cal AD 1080–1740 (870–210 cal BP; 95.4% probability). As such, we have chosen to describe this phase of activity as simply 'Historic'. The radiocarbon determinations were shown to be statistically consistent (χ^2-test: Df = 1, T = 2.9, 5% = 3.8), suggesting the possibility of a single depositional event which their posterior density estimates indicate may have been centred on *c* cal AD 1200 (*c* 740 cal BP; 95.4% probability; Table 4).

The average sedimentation rates was calculated to be a minimum of 0.02cm/year between *c* cal AD 530 (*c* 1420 cal BP; 95.4% probability) to *c* cal AD 1740 (*c* 210 cal BP; 95.4% probability; Table 5).

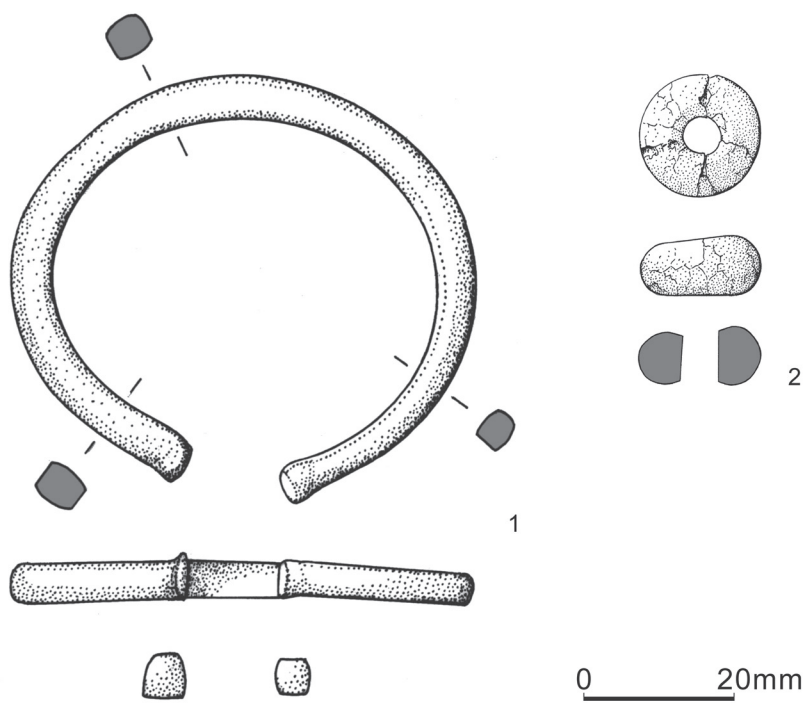

ILLUS 11 The bracelet and amber bead from Croig Cave Context 108

ARTEFACTS

Trevor Cowie and Brendan O'Connor

IRON RUN SLAG

A fragment of run slag, 62mm × 26mm × 35mm was recovered from within CC103 at a depth of 100–110cm (illus 10). Slag of this density, and with a distinctive 'ropey' appearance, is characteristic of material allowed to run from a furnace, often called 'tapped' slags. Although such material is often indicative of smelting (Starley 2002), not all slags with a 'run' appearance, particularly small pieces like this example, are necessarily associated with this process and it could simply be a product of iron-smithing (Andrew Heald pers comm).

PENANNULAR COPPER ALLOY BRACELET

A complete penannular bracelet (illus 11) was recovered from within a small pit (CC107 and CC108), within which the amber bead was also found. The bracelet is 61mm × 55mm, externally and 50.5mm × 45mm internally. The hoop has a width of 4.1 to 5.5mm and a thickness of 4.1 to 5.5mm. Its weight prior to conservation was 25.03g. Extensive dark green corrosion obscures a paler green underlying surface.

The hoop is out of shape and does not lie flat. Its sides are flat with well-defined angles; its inner and outer surfaces are slightly curved. The section is irregular, varying from D-shape with flattish internal face to a more oval form, which appears to be a consequence of manufacture rather than wear. The terminals have not been properly aligned and point in slightly different directions. Both terminals are slightly thickened with a perceptible expansion on both outer faces and on one side. Although the faces of the terminals are both of squarish form, they do not match in size. Overall, the features of the bracelet suggest that it was made as a bar and bent into shape rather than having been directly cast in a penannular form.

TABLE 6
Elemental analysis of the slag, bracelet and surface corrosion products (all concentrations in µg/kg; the lowest limit of detection was 40µg/kg)

Sample	*U*	*Pb*	*As*	*Cu*	*Fe*	*Hg*	*Se*	*Zr*	*Ni*	*Mn*
Slag	<LLD	3075	665	<LLD	549500	147	43	1348	3505	2756
Metal scrap 1	953	36937	4819	900843	6731	<LLD	<LLD	<LLD	<LLD	<LLD
Metal scrap 2	646	42208	3526	945363	4615	<LLD	<LLD	<LLD	<LLD	<LLD
Metal scrap 3	307	39877	1446	956594	3912	<LLD	<LLD	<LLD	<LLD	<LLD
Corrosion products 1	649	34654	2397	548931	1244	<LLD	<LLD	<LLD	<LLD	<LLD
Corrosion products 2	418	33301	2415	572405	4422	<LLD	<LLD	<LLD	<LLD	<LLD
Corrosion products 3	643	8137	418	111598	1610	<LLD	<LLD	<LLD	<LLD	<LLD

TABLE 7
Lead isotope analysis of the slag, bracelet and surface corrosion products

Sample	$^{208}Pb/^{204}Pb$	$^{207}Pb/^{204}Pb$	$^{206}Pb/^{204}Pb$	$^{208}Pb/^{206}Pb$	$^{207}Pb/^{206}Pb$
Slag	38.5636±0.0002	15.6323±0.0002	18.4522±0.0002	2.0899±0.0002	0.8472±0.0004
Metal scrap 1	38.0157±0.0002	15.2964±0.0002	18.1657±0.0002	2.0927±0.0005	0.8421±0.0005
Metal scrap 2	38.0167±0.0003	15.2952±0.0003	18.1876±0.0002	2.0902±0.0004	0.8410±0.0003
Metal scrap 3	38.0178±0.0001	15.2935±0.0003	18.1757±0.0002	2.0917±0.0005	0.8414±0.0005
Corrosion products 1	38.0223±0.0002	15.2433±0.0002	18.0506±0.0002	2.1064±0.0004	0.8445±0.0004
Corrosion products 2	38.0116±0.0002	15.2427±0.0001	18.0716±0.0002	2.1034±0.0005	0.8435±0.0005
Corrosion products 3	38.0216±0.0004	15.2366±0.0004	18.0782±0.0002	2.1032±0.0004	0.8428±0.0003

Bronze penannular bracelets with expanded terminals form a significant component of a number of well-known Late Bronze Age hoards, mainly from north-east Scotland and including Braes of Gight (Coles 1960: 94–5, pl II.2), Rehill (ibid, 97) and Glentanar (Pearce 1971, 1976) all in Aberdeenshire; Balmashanner in Angus (Coles 1960: 98; Schmidt & Burgess 1981: pl. 152B) and Auchtertyre in Moray (Coles 1960: 120). To these must be added the significant group of bracelets recovered during excavations at the Sculptor's Cave, Covesea, again in Moray (Benton 1931; Shepherd 2007). In Fife, bracelets form a major element of the large ornament-dominated hoard discovered in Priestden Place, St Andrews (Cowie et al 1991). In southern Scotland, bracelets occur more sporadically but mention may be made of the fragment of a bronze bracelet from the Late Bronze Age settlement at Traprain Law, East Lothian (Burley 1956: 150).

The bracelets fall into two main varieties: the Covesea type has terminals expanded outwards only, while the other (often simply called the Irish type) has terminals expanded all the way round (Coles 1960: 39–41). Although the general form of the Croig Cave bracelet compares readily enough with other Late Bronze Age bracelets found in Scotland, it differs in several respects. While perceptibly thickened, the rather crude manufacture and unevenness of the terminals contrasts with the quality of the finish of other examples; similarly, the rather irregular angular section of the Croig Cave specimen stands in quite marked contrast to the usual neat round D-shaped cross section. Flattening of sides does occur, notably on some of the bracelets from Braes of Gight (NMS: acquisition DQ 282–283; Coles 1960: 94–5), but those examples typically have a better finish. One factor may have been that, while many penannular bracelets were cast in their near final form, the Croig Cave example appears to have been manufactured by bending a bar into shape. Taken together, these differences raise the possibility of inferior workmanship or, though less likely, that the Croig Cave bracelet

is an unfinished piece. Whether the hoop has been twisted out-of-true as a result of use or deliberate damage at the time of deposition is unknown. Even if not a typical example, the form of this penannular bracelet with expanded ends indicates a date within the Ewart Park phase of the Late Bronze Age (see below).

AMBER BEAD

The bead was recovered whole (illus 11) but was badly cracked and fell apart immediately following excavation. As a result of skilful conservation by Jane Clark (National Museum of Scotland, Department of Conservation & Analytical Research) it has been reassembled almost complete with only a few tiny chips missing. The bead is 16.5mm in diameter and 7–8mm in thickness. All external surfaces are a light orange-brown, matt and highly cracked and crazed when seen under magnification. Below the friable outer surface, the exposed core was in better condition, translucent orange and glossy (with the familiar 'barley sugar' quality associated with amber). The bead is circular in outline with a central perforation which appears slightly narrower at one end than the other. No traces of manufacture could be observed before analysis because of the crazing of the surface, so it remains uncertain whether the perforation was bored from just one direction or both. It has convex sides with straight faces which converge slightly to give a wedge-shaped section.

Prehistoric amber from Britain is ultimately of Baltic geological origin, though such Baltic amber does occur naturally in eastern Britain (Beck & Shennan 1991: 37), but the location of Croig Cave in the west of Scotland suggests that the amber bead could, alternatively, have been brought from Ireland (cf Briggs 1997)

The wedge-shaped cross-section of the bead is characteristic of Late Bronze Age amber beads throughout Britain (Beck & Shennan 1991: 57, Group 4, figure 41). Wedge-shaped beads occur in the Scottish hoards of the Ewart Park metalworking phase from Adabrock, Lewis, Balmashanner, Angus, and St Andrews, Fife. Balmashanner is the largest group, 26 beads (NMS acquisition 167–92; Coles 1960: 98–9; Beck & Shennan 1991: 184–5, figure 11.20, 4). Both Adabrock beads (NMS acquisition DQ 223–4; Coles 1960: 127; Beck & Shennan 1991: 184, figure 11.19.2) are distinctly wedge-shaped. The beads from the St Andrews hoard, referred to previously, are all slightly wedge-shaped (Cowie et al 1991: 53). The beads in the Glentanar hoard, Aberdeenshire, are too fragmentary for confident comparison, but one appears to have been wedge-shaped (NMS acquisition DQ 397; Pearce 1976: 124, figure 1, 1; Beck & Shennan 1991: 188). The amber beads found with the bronze bracelets mentioned above in the Sculptor's Cave (NMS acquisition 1931.1069–72; Benton 1931; Beck & Shennan 1991: 186, figure 11.20, 2) are not wedge-shaped.

South of the border, the single amber bead from Heathery Burn Cave, Co Durham, is slightly wedge-shaped (Beck & Shennan 1991: 172, figure 11.12, 6), while most of the 30-odd beads that may be part of a necklace from an unpublished find at High Throston, in the same county, are also wedge-shaped. The Ewart Park hoards from Ty Mawr and Llangwyllog on Anglesey both contain wedge-shaped examples among their amber beads (ibid: 192–3, figure 11.23, 1–2; Lynch 1991: figures 68, 19 and 69, 15–18). In southern England, wedge-shaped amber beads occur in Late Bronze Age contexts at Runneymede Bridge, Berkshire (Longley 1980: 31–2, figure 18, 69–70; Beck & Shennan 1991: 168, figure 11.10, 2; Needham & Spence 1996: figure 101, AM2), and Potterne, Wiltshire (Beck & Shennan 1991: 166–7, figure 11.24).

The larger number of amber beads from Ireland embraces a wider variety of shapes than found in Britain, but wedge-shaped beads occur in the following Late Bronze Age hoards: Mountrivers, Co Cork (Eogan 1983: 77, figure 38, 3), Killcreen West, Co Fermanagh (ibid: 86, figure 41D, 3), near Portlaoise, Co Laois (ibid:

101, figure 55, 58), Banagher, Co Offaly (ibid: 116, figure 63, 5), and Rathinaun, Co Sligo (ibid: 152, figure 84, 27–54).

DISCUSSION

The Croig bracelet and bead represent a discovery of considerable interest for a number of reasons. First, finds of Bronze Age metalwork from excavated contexts are by no means common in northern Britain, while those from dated contexts are even rarer. The available radiocarbon date for the context is wholly in keeping with the expected range for Ewart Park metalwork, *c* 1020–800 cal BC (following Needham et al 1997). Regionally, the little group from Croig Cave therefore forms an important addition to the inventory of finds from an area of Argyll with very little in the way of recorded Late Bronze Age material. Finally, it adds to the small but significant number of Late Bronze Age deposits from caves in Scotland, which themselves form part of a wider north-west European tradition.

As first noted by Sylvia Benton, the excavator of the Sculptor's Cave, Covesea (1931), the distribution of bronze bracelets in Scotland is predominantly eastern. By contrast, bronze bracelets are rare in the west, where bracelets of comparable form tend to be of gold (Coles 1960; Hawkes & Clarke 1963: 235–6; O'Connor 1980; Eogan 1994: figures 38–9). The Croig discovery once again raises questions about the nature of the known archaeological record in certain regions of Scotland, where the quantity of metalwork in circulation may be belied by the sparse inventory of surviving finds. While this may be partly due to the relative lack of fieldwork, it may also reflect patterns of deposition in antiquity. A find germane to this problem is the discovery at Cladh Hallan, South Uist, of fragments of clay moulds for casting rings or bracelets (Parker Pearson et al 2004) – indicating that despite being unrepresented or under-represented in the surviving inventory of metalwork, some artefact types were being produced and presumably circulated in the west of Scotland. Seen in this light, despite being rather cruder manufacture than usual (among the surviving inventory of finds), the Croig bracelet fits in with a wider picture; penannular bracelets, culling ideas from Irish and continental sources, were probably widespread in Scotland during this phase of the Late Bronze Age. Amber, too, was clearly circulating widely at this time – and penannular bronze bracelets and amber beads regularly occur in association in hoards (eg at Glentanar, Aberdeenshire; Balmashanner, Angus; St Andrews, Fife, already referred to above) and in the deposits from Sculptors Cave, Covesea, itself.

Locally, the finds from Croig Cave are a significant addition to the otherwise sparse scatter of Late Bronze Age artefacts from Mull and the immediate region of mainland north Argyll and its other offshore islands. No recorded finds of Late Bronze Age metalwork are known from Mull itself (RCAHMS 1980); however, at least two separate discoveries of bronze swords are known from the vicinity of Breachacha on Coll, while a further sword is recorded from Tiree (McGillivray 1876–8; Anon 1905), but all remained in private hands and all are now lost. However, part of a sword blade, recently found at Breachacha on Coll, may represent the modern rediscovery of part of one of the earlier finds (Cowie 2006). A copper-alloy penannular ring of the type known as hair rings or ring money was discovered at Torastan on Coll (Beveridge 1903). For completeness, it should be noted that a gold ornament hoard, once thought to be from Torloisk on Mull, has been shown to have been found in Southern Ireland and should be discounted (Eogan 1967; see now also Cahill 2006).

However, the quantity of metalwork in circulation in the north Argyll area may be by the scarcity of surviving finds. If viewed as part of a wider province, linked by the sea as much as by the land, the relative

sparseness of material in the immediate region is balanced by the richer inventory of Late Bronze Age finds from mid-Argyll, Kintyre and Islay to the south, and from the Small Isles and Skye to the north. Across this wider region too, a number of finds of gold bracelets and cup-ended ornaments, mostly now unfortunately lost, again hint at contacts with Ireland during this period (Eogan 1994: figures 39–40).

Deposition of Late Bronze artefacts within caves can be paralleled, albeit on a larger and more spectacular scale, at the well-known sites of Sculptor's Cave in Moray (Benton 1931), and Heathery Burn, Durham (Britton & Longworth 1969). Shepherd (2007) has effectively set such discoveries in the wider context of Late Bronze Age activity in caves in north-west Europe.

LEAD ISOTOPE COMPOSITION OF THE BRACELET AND SLAG

Stuart Black

The Pb isotopic data and major trace element data pertaining to the bracelet are presented in Tables 6 and 7. The bracelet is identified as an arsenical, leaded, copper alloy (arsenic 0.1–0.48wt%; iron 0.39–0.67wt%; lead 3.7–4.2wt%; copper 90–95.6wt%). The corrosion products show typically less elemental copper, but similar concentrations of lead and other elements to the metal scrapes, indicating extensive surface alteration of the copper. This is evident in the large malachite ($CuCO_3$) deposition in the surface and an altered pale green copper surface (CuO). Both of these alteration products are due

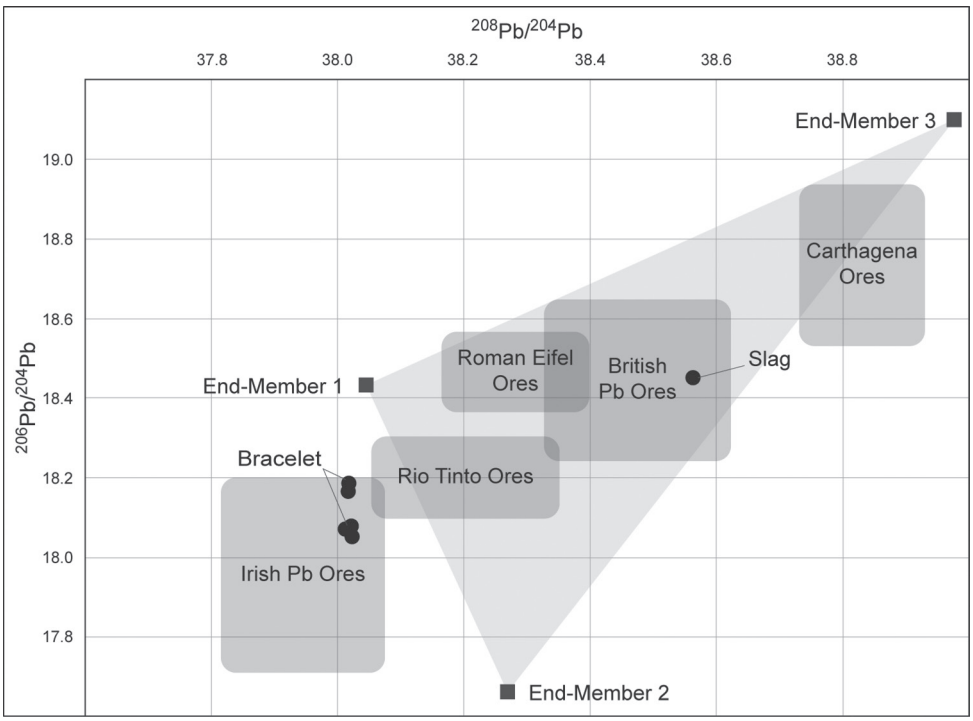

ILLUS 12 $^{208}Pb/^{204}Pb$ – $^{206}Pb/^{204}Pb$ diagram with measured Pb isotopic composition of the common products and metal scrapes from the bracelet and showing potential effect of mixing on the isotopic composition of the materials

to interaction with carbonates and water from the midden deposit.

Illustration 12 shows a $^{208}Pb/^{204}Pb$–$^{206}Pb/^{204}Pb$ diagram with the measured Pb isotopic composition of the corrosion products and metal scrapes from the bracelet. The bracelet corresponds to a field associated with the Irish ore fields, assuming that its lead component

TABLE 8
Semi-quantitative XRD results showing the bulk mineralogy of the sediment matrix

Sample	*Smectite*	*Gypsum*	*Kaolinite*	*Quartz*	*Anorthite*	*Calcite*	*Hematite*
PHASE 3: HISTORIC							
CCBS:1	major	minor	trace	minor	major	major	trace
CCBS:2	minor	absent	minor	minor	minor	major	minor
CCBS:3	major	trace	absent	minor	major	minor	minor
PHASE 2: IRON AGE							
CCBS:4	major	trace	trace	trace	major	major	minor
CCBS:5	minor	trace	trace	trace	minor	major	trace
CCBS:6	trace	trace	trace	minor	minor	major	trace
CCBS:7	minor	absent	trace	trace	major	major	minor
CCBS:8	minor	absent	minor	minor	minor	major	minor
CCBS:9	minor	trace	minor	minor	minor	major	minor
CCBS:10	minor	absent	minor	minor	major	major	minor
PHASE 1: BRONZE AGE							
CCBS:11	minor	trace	minor	minor	minor	major	minor
CCBS:12	minor	absent	major	minor	minor	major	minor
CCBS:13	major	trace	minor	minor	minor	major	minor
CCBS:14	minor	absent	minor	minor	minor	minor	minor
CCBS:15	minor	absent	minor	minor	minor	major	minor
CCBS:16	major	trace	minor	minor	minor	minor	minor
CONTROLS							
CCBS:17	minor	trace	minor	minor	minor	major	minor
CCBS:18	trace	absent	trace	trace	minor	major	minor

has derived from a single source rather than from mixed deposits, an issue further discussed below. There are several Pb and Zn ore deposits in the Irish Midlands (Andrew et al 1986), the largest ones being at Navan (>70Mt), Lisheen (>20 Mt) and Silvermines (>18 Mt) (Johnstone 1999). Mining of these deposits started around the 1960s, but there is archaeological evidence for an important centre of pre-medieval metal working in Southern Ireland (Co Kerry). Mining of polymetallic deposits was common in this region, with copper being a particularly good example. Copper mining started in Ireland around 4500 BP and copper tools with signatory high As, Sb and Ag contents were produced from the smelting process (O'Brien 2004). The bracelet also contains a high concentration of arsenic (0.1–0.48wt%) and silver (up to 4800μg/kg) which supports the association with the Irish ore fields.

The sample of slag shows isotopic and trace element compositions that contrast markedly with the copper bracelet. Its Pb isotopic composition plots in the middle of the British Pb ore field and its lacks any detectable copper or uranium. This confirms that it is not a copper slag and most likely to be an iron tap slag: it has no relationship in terms of source and material process with the bracelet. The presence of trace elements not detected within the bracelet, namely Hg, Se, Zr, Ni and Mn, further supports this lack of any association between the slag and the bracelet.

Illustration 12 also shows the potential effect of mixing on the isotopic composition of the materials. The more mixtures an object represents, the more likely it is to migrate towards a multi-component field in the central portion of the diagram. An example of a three component-mixture is given with three end members (1, 2 and 3), providing mixing relationships inside the large triangle on illus 11. This serves to show that end-member compositions are important in determining final compositions of mixtures, and hence materials plotting on the periphery of the diagram, such as the samples from the bracelet, are unlikely to represent significant mixtures of ore sources as they have an extreme isotopic composition. The slag, however, does plot in the middle part of the diagram and has the potential to have originated from multiple sources.

SEDIMENTARY ANALYSIS

X-RAY DIFFRACTION

XRD patterns were produced for the <2mm fraction of bulk samples (CCBS:1 to CCBS:16) and controls (CCBS:17 and CCBS:18); the semi-quantified results are provided in Table 8. The sediment matrix was comprised of six different minerals which were categorised according to their contribution to the bulk mineralogy of each sample as follows: Absent, representing 0% of the bulk mineralogy; Trace, less than 5%; Minor, between 5–25%; and Major representing more than 25% of the bulk mineralogy.

The diffraction patterns contain numerous high peaks relating to calcite and to a lesser extent, anorthite, with low peaks relating to quartz, hematite and gypsum. Calcite is the major mineral component in 13 of the samples, with the exception of CCBS:3, CCBS:14 and CCBS:16, where it represents a minor proportion (Table 8). Calcite ($CaCO_3$) is the primary constituent of the shells of marine organisms. As such, it is likely that its high frequency presence within the sediments derives from the limpet and periwinkle shells that form the main structural elements of the midden.

Peaks due to anorthite constitute a major component of the bulk mineralogy in CCBS:1, CCBS:3–4, CCBS:7 and CCBS:10. Anorthite ($CaAl_2Si_2O_8$) is the calcium end-member of weathered plagioclase feldspar occurring in mafic igneous rock such as basalt. Tertiary basalt lavas form the predominant solid geology of the northern massif, a geological region of Mull comprising the Plateau Group of igneous rocks. As such, the elevated levels of anorthite

TABLE 9
Major element composition of the sediment matrix (wt%)

Sample	*Na_2O*	*MgO*	*Al_2O_3*	*SiO_2*	*P_2O_5*	*K_2O*	*CaO*	*TiO_2*	*MnO*	*Fe_2O_3*	*LOI*	*Total*
PHASE 3: HISTORIC												
CCBS:1	1.35	5.00	7.74	33.88	4.43	0.56	15.30	1.54	0.41	16.73	3.58	89.87
CCBS:2	1.20	5.63	8.57	34.36	3.55	0.52	16.70	1.75	0.40	18.58	3.52	94.49
CCBS:3	1.58	7.70	9.48	44.91	1.44	0.74	9.19	1.82	0.58	19.28	3.57	100.37
PHASE 2: IRON AGE												
CCBS:4	1.25	6.88	7.99	36.62	2.97	0.49	17.48	1.52	0.40	16.90	3.96	95.59
CCBS:5	1.02	4.44	5.16	22.74	2.05	0.31	34.74	1.23	0.34	12.81	3.39	86.95
CCBS:6	0.94	3.28	4.21	19.51	0.85	0.21	41.57	1.19	0.23	11.58	3.70	86.04
CCBS:7	1.24	3.94	5.41	24.40	0.78	0.31	35.30	1.49	0.20	12.05	4.13	88.62
CCBS:8	0.98	3.65	5.59	25.05	1.31	0.24	35.12	1.40	0.23	12.41	4.05	89.14
CCBS:9	1.24	4.16	6.75	29.12	1.65	0.26	29.19	1.54	0.28	13.64	4.37	91.52
CCBS:10	1.21	4.91	7.29	33.12	1.31	0.34	25.91	1.67	0.27	14.91	3.58	97.74
PHASE 3: BRONZE AGE												
CCBS:11	1.07	5.48	8.93	37.49	1.83	0.32	21.47	1.53	0.27	16.18	3.35	94.64
CCBS:12	1.01	6.18	9.91	45.71	0.46	0.17	10.06	1.63	0.22	17.39	3.85	104.48
CCBS:13	1.09	6.56	10.85	51.35	0.25	0.17	9.12	1.76	0.20	18.59	4.14	97.52
CCBS:14	1.17	6.29	11.01	49.46	0.88	0.27	9.67	1.84	0.26	18.54	3.34	105.52
CCBS:15	1.03	6.35	11.06	50.85	0.26	0.20	9.36	1.83	0.20	18.33	3.44	105.00
CCBS:16	0.99	5.93	11.80	53.21	0.12	0.18	7.85	2.01	0.17	17.63	3.34	105.95
CONTROL SAMPLES												
CCBS:17	1.26	5.44	12.83	39.20	1.76	0.40	14.07	1.60	0.33	15.43	3.78	92.32
CCBS:18	1.35	4.25	2.53	6.74	0.12	0.02	64.62	0.42	0.10	3.00	3.93	83.15
INTERNATIONAL STANDARD VALUES												
GSP-1	2.49	0.70	14.91	73.71	0.25	5.57	1.91	0.62	0.04	3.85	0.70	104.05
DRN	2.72	4.55	18.28	58.44	0.25	1.79	7.34	1.06	0.22	10.13	2.35	104.78

in these samples are likely to derive from the build-up of weathered rock minerals deriving from the interior basalt walls and ceiling of the cave.

A feasible interpretation is that those samples enriched with weathered basalt indicate periods during which the cave was less intensively used: a reduction in the rate of midden formation would provide an opportunity for weathered minerals to accumulate in the absence of calcitic inputs from marine shells. Furthermore, during periods of low activity, limited trampling of deposits would permit distinct layers of weathered minerals to form on the surface of the cave floor. This conclusion is supported by the stratigraphic position of the samples with elevated levels of anorthite (illus 4): CCBS:1 corresponds with the modern surface of the midden (top of Phase 3); CCBS:3 and CCBS:4 were collected from the upper surfaces of CC102a and CC102b respectively, representing the transitional zone between Phase 2 and Phase 3; CCBS:7 corresponds with the upper surface of CC103a (mid Phase 2), while CCBS:10 was taken from the upper surface of CC103b (lower Phase 2).

Peaks due to clays in the smectite group (2:1 lattice clay minerals), such as

TABLE 10
Major element composition by weight percent of geological reference material held by School of Human and Environmental Science, University of Reading (wt%)

Reference sample	Na_2O	MgO	Al_2O_3	SiO_2	P_2O_5	K_2O	CaO	TiO_2	MnO	Fe_2O_3
GRANITES										
G1 Granite (ZN205)	3.32	0.38	14.04	22.64	0.09	5.48	1.39	0.26	0.03	1.44
G2 Granite (ZN85)	4.07	0.76	15.40	69.22	0.13	4.46	1.96	0.46	0.03	2.69
Granite (ZN50)	3.36	0.06	12.08	75.70	0.01	4.99	0.78	0.09	0.02	2.02
Nim G (ZN54)	3.36	0.06	12.08	75.70	0.01	4.99	0.78	0.09	0.02	2.02
S16 (ZN54)	3.30	0.14	11.30	67.12	0.08	4.26	8.85	0.10	0.02	0.59
MA-N (ZN220)	5.84	0.04	17.02	66.70	1.39	3.18	0.59	0.01	0.04	0.47
BASALTS										
BCR-1 (ZN 187)	3.27	3.45	13.63	54.55	0.36	1.70	6.97	2.26	0.18	13.41
BR (ZN150)	3.08	13.28	10.20	38.20	1.04	1.40	13.80	2.60	0.20	12.88
BE-N (ZN120)	3.18	13.15	10.07	38.20	1.05	1.39	13.87	2.61	0.20	12.84
JB1 (ZN84)	2.79	7.73	14.53	52.17	0.26	1.42	9.29	1.34	0.16	8.97
JB2 (ZN103)	2.03	4.66	14.67	53.00	0.10	0.43	9.89	1.49	0.20	14.34
JB3 (ZN103)	2.82	5.20	16.89	51.00	0.29	0.80	9.86	1.45	0.13	11.88
BHU0-1 (ZN105)	2.29	7.31	13.85	49.90	0.28	0.54	11.3	2.69	0.17	12.23

montmorillonite, occur in all samples ranging from a major component (CCBS:1, CCBS:3, CCBS:4, CCBS:13 and CCBS:16) to traces (Sample CCBS:6). Montmorillonite has been recorded as the initial weathering product of plagioclase in basalt in various environments (Singer 1970, 1973; Lunkad & Raymahashay 1978). Furthermore, the predominance of montmorillonite in the fine fraction of basalt in Morvern, in the north-west of Scotland, has been reported previously by Bain et al (1980). Its presence is likely to derive from a process of basalt diminution to a state where the original basalt is completely destroyed. Although differentiating the sources of end-members of geological weathering is problematic, minor and trace peaks due to kaolinite, silica (as quartz) and hematite indicate that the bulk of the sediment contains an intimate mixture of clays with Si- and Fe-bearing minerals in relative proportions typical of weathered basalts (ibid).

Trace peaks due to gypsum ($CaSO_4 \cdot 2H_2O$) occur in CCBS:3 CCBS:6, CCBS:9, CCBS:11, CCBS:13 and CCBS:16, while the XRD pattern for CCBS:1 indicates its presence as a minor component. Gypsum is a soft sulphate mineral – composed of calcium sulphate dehydrate – and its presence in the sediment matrix is to be expected due to the proximity of the cave to marine influences; sea water naturally contains dissolved gypsum so relatively low levels are likely to be deposited in salt spray from the shore.

Control sample CCBS:17, collected from the interior floor of the cave, produced XRD peaks corresponding with the array of minerals present in the sediment matrix of the midden at roughly the same proportions. Control sample CCBS:18, collected from the foreshore, was enriched with calcite and anorthite but had lower quantities of clay minerals to CCBS:17 coming from within the cave. This indicates that the sediment matrix was mainly comprised of autochthonous minerals. The lack of gypsum from sea water in the beach sediments may be a result of its dissolution in rain water.

X-RAY FLUORESENCE (XRF)

Table 9 provides the results of XRF analysis presented as major elements represented by their oxides as weight percentages, along with LOI measurements, international standard values and total elemental composition. Table 10 provides the range of major element values common to two different rock types, basalt and granite, both found on the Isle of Mull, based on XRF data obtained from standard geological reference material held at the University of Reading.

Major elements

The XRF data demonstrates that the elemental composition of the sediment matrix is dominated by silica (SiO_2) and calcium oxide (CaO), with values ranging from a minimum of 19.51wt% (CCBS:6) to a maximum of 53.21wt% (CCBS:16), and from a minimum of 7.85wt% (CCBS:16) to a maximum of 41.57wt% (CCBS:6), respectively (Table 9). Basaltic rocks typically contain *c* 45–55 wt% SiO_2 and tend to be enriched with iron (Fe), magnesium (Mg) and calcium (Ca), with low values of potassium (K) and sodium (Na); granites tend to contain significantly higher proportions of SiO_2 (65–75wt%), K and Na with low values of Fe, Mg and Ca (Table 10). The SiO_2 content of the Croig Cave samples, therefore, more closely matches that of the basalt standards, particularly in CCBS:3 and CCBS:12 to CCBS:16 with values ranging from 44.91–53.21wt%. Table 9 shows that the proportions of SiO_2 and CaO change over time, which is likely to be linked to usage patterns of the cave. Levels containing lower values of SiO_2 (Samples 4–11) exhibit an increase in CaO that corresponds with the changing proportions of marine shell in the midden deposits (see below). In these levels, CaO is likely to derive predominantly from calcium-containing inorganic materials, such as the marine shells, although some indeterminate proportion will also be derived from the bedrock geology.

TABLE 11
Trace element composition of the sediment matrix (ppm)

Bulk sample	*V*	*Cr*	*Co*	*Ni*	*Cu*	*Zn*	*Pb*	*Rb*	*Sr*	*Y*	*Zr*
PHASE 3: HISTORIC											
CCBS:1	237.5	68.5	53.0	46.5	171.0	4657.5	176.0	21.5	791.0	31.0	112.0
CCBS:2	263.5	70.5	58.5	48.0	137.0	722.0	88.0	20.5	766.0	38.0	143.5
CCBS:3	281.5	37.0	72.5	44.5	85.0	1436.0	46.5	14.5	510.0	42.0	141.0
PHASE 2: IRON AGE											
CCBS:4	243.0	36.0	65.5	41.0	82.5	794.5	57.5	14.0	788.5	34.5	115.0
CCBS:5	189.0	40.5	46.0	40.5	112.5	2247.0	54.0	*	1405.5	31.0	74.5
CCBS:6	181.5	42.5	42.5	40.0	130.0	985.5	74.0	*	1439.0	25.0	63.5
CCBS:7	214.5	43.0	45.5	42.0	94.5	864.0	38.0	*	1227.0	31.0	104.5
CCBS:8	200.5	55.0	42.5	44.5	89.0	157.5	53.5	*	1253.0	24.0	85.0
CCBS:9	224.5	36.0	43.5	40.0	111.0	156.5	36.5	8.5	1149.0	27.5	93.5
CCBS:10	209.5	36.0	58.0	47.0	115.0	163.5	45.0	9.0	719.5	30.0	119.5
PHASE 1: BRONZE AGE											
CCBS:11	233.0	29.5	52.5	42.0	99.0	120.5	37.0	9.5	835.5	37.0	119.5
CCBS:12	244.0	31.0	64.0	50.0	75.0	108.0	45.5	*	304.5	33.5	152.0
CCBS:13	206.5	28.5	66.0	43.0	48.0	98.5	23.0	*	264.5	26.5	118.5
CCBS:14	218.0	32.5	69.5	50.5	65.5	100.0	28.5	*	245.0	30.0	140.0
CCBS:15	222.5	32.0	65.5	53.5	72.5	101.5	53.5	*	229.5	27.0	143.0
CCBS:16	229.5	30.5	60.0	49.5	65.0	366.0	33.0	*	197.5	25.0	153.5
CONTROL SAMPLES											
CCBS:17	201.0	20.0	67.0	48.0	56.0	90.0	5.0	*	358.0	28.0	103.0
CCBS:18	81.0	9.0	7.0	14.0	31.0	34.0	14.0	–6.0	2563.0	7.0	*
INTERNATIONAL STANDARD											
GSP-1	72.0	*	10.0	10.0	29.0	97.0	77.0	255.0	226.0	39.0	511.0
DRN	233.0	52.0	31.0	17.0	53.0	147.0	64.0	78.0	421.0	31.0	152.0

* Below detectable limits

Relatively high proportions of iron oxide (Fe_2O_3), ranging from 11.58–19.28wt%, correspond well with the values for Fe_2O_3 in the basalt reference material, with the highest values in excess of 15wt% recorded in CCBS:2 to CCBS:4 and CCBS:13 to CCBS:14. High values of iron oxide are to be expected given the presence of hematite indicated by the XRD data throughout the sequence. High values of magnesium oxide (MgO), ranging from a minimum value of 3.28wt% to a maximum of 7.70wt%, also fall within the range recorded in the basaltic reference materials, exhibiting overall consistency with the Total Alkali Silica (TAS) classification of igneous rock (Le Maitre et al 2002). Furthermore, enrichment with respect to Fe_2O_3, and to a lesser extent MgO and manganese oxide (MnO), in CCBS:3 is of particular interest, indicating that this level represents a geochemical threshold in the matrix environment, perhaps relating to chemical weathering and the formation of a zone of iron pan above the main accumulation of shells (represented by CCBS:4 to CCBS:11).

Proportions of aluminium oxide (Al_2O_3) and titanium dioxide (TiO_2) tend to be at their lowest in the levels enriched with CaO (CCBS:5 to CCBS:11). This indicates that differences occur in the proportions of weathered material contained in the sediment matrix. The tendency for Fe_3O_2, TiO_2 and Al_2O_3 to accumulate in more weathered basalt samples has been reported previously in western Scotland by Bain et al (1980). This provides additional supporting evidence to suggest that the period of most intense activity within Croig Cave is represented in those levels from where CCBS:4 to CCBS:11 were collected as these contain the lowest quantities of end members of weathered basalt. Furthermore, the composition and proportions of elemental oxides in control sample CCBS:17 are similar to those of CCBS:1 to CCBS:3 and CCBS:12 to CCBS:16, providing evidence for the accumulation of autochthonous sediments with the main allochthonous formation due to marine shell inputs occurring between CCBS:4 to CCBS:11, these being enriched in CaO. Control sample CCBS:18 further substantiates this as its composition is dominated by CaO typical of beach deposits under strong marine influences.

Trace elements

Trace element composition values for a standard range of elements in the sediment matrix are provided in Table 11. This shows that all of the samples are enriched with strontium (Sr) with values ranging from a minimum of 197.5ppm in CCBS:16 to 1439.0 ppm in CCBS:6. The lowest values are found in CCBS:12 to CCBS:16, with numbers rising as shell content increases with values remaining high (>500ppm) in the upper levels. Sr is an abundant dissolved constituent in seawater. Its presence in the sediment matrix is likely to derive from the shells contained therein as it can precipitate in marine carbonates and is a direct reflection of seawater during the lifespan of the mollusc (McArthur et al 2001). It is to be expected, therefore, that the highest levels of Sr (>2560ppm) were detected in control sample CCBS:18 this being taken from littoral sediments likely to contain high inputs of marine shells.

An unexpected result was the exceedingly high levels of zinc (Zn) in CCBS:1 at 4657.5ppm and to a lesser extent, its enrichment (>720ppm) in CCBS:2 to CCBS:7. At these levels, the source of Zn is unlikely to be wholly autochthonous from basalt inputs and must represent a derivative of allochthonous material. This raises the prospect that seaweed may have been deliberately deposited in the midden as marine vegetation contains high levels of Zn (Lunde 1970). Values of phosphate (P_2O_5) are also elevated above the average for basalt in these levels (Table 10), which could indicate inputs of burnt seaweed (Stuart Black pers comm). The possibility of burnt seaweed inputs is substantiated by

TABLE 12
Particle size distributions (weight, g) of sediment matrix bulk samples

Bulk sample	*64mm (–6ϕ)*	*31.5mm (–5ϕ)*	*16mm (–4ϕ)*	*8mm (–3ϕ)*	*4mm (–2ϕ)*	*2mm (–1ϕ)*	*1mm (–0ϕ)*	*500μm (1ϕ)*	*Total*
PHASE 3: HISTORIC									
CCBS:1	0.0	277.6	487.0	557.9	497.5	338.8	326.4	92.0	2577.2
CCBS:2	0.0	320.2	255.6	267.0	187.4	221.8	144.4	34.0	1430.4
CCBS:3	304.9	727.7	108.8	1017.5	758.1	705.6	467.6	104.3	4194.5
PHASE 2: IRON AGE									
CCBS:4	0.0	578.5	744.4	492.7	377.2	457.0	338.4	68.8	3057.0
CCBS:5	0.0	268.9	258.3	209.6	159.2	310.6	187.6	14.2	1408.4
CCBS:6	0.0	0.0	0.0	63.8	67.2	121.8	74.0	7.6	334.4
CCBS:7	0.0	137.4	99.7	115.7	100.9	152.8	104.8	33.4	744.7
CCBS:8	0.0	152.7	291.6	220.7	224.0	376.0	292.4	22.6	1580.0
CCBS:9	0.0	0.0	330.2	396.7	363.4	595.0	373.2	34.1	2092.6
CCBS:10	0.0	420.9	662.3	698.4	525.9	590.8	462.8	14.6	3375.7
PHASE 1: BRONZE AGE									
CCBS:11	0.0	71.3	323.3	498.0	425.7	576.8	437.2	17.7	2350.0
CCBS:12	0.0	0.0	47.7	190.9	391.9	718.8	886.0	482.5	2717.8
CCBS:13	0.0	0.0	217.0	659.3	737.3	423.4	846.8	579.2	3463.0
CCBS:14	0.0	234.4	792.4	1240.6	1011.7	941.8	768.4	273.8	5263.1
CCBS:15	0.0	0.0	354.8	961.7	1058.7	339.8	679.6	355.6	3750.2
CCBS:16	365.9	869.8	624.1	923.5	728.5	835.4	805.6	118.8	5271.6

correspondingly high magnetic susceptibility and quantities of charcoal (see below) in the upper levels of the sequence.

Seaweed may have been brought into the cave for consumption, as an incidental product of coastal foraging or relating to a process linked to kelping industries. Burning seaweed was once the main method of obtaining impure forms of sodium carbonate (Na_2CO_3), also known as 'soda ash' (Morand et al 1991). The suggestion that zinc-rich biological material was deliberately deposited in the midden is supported by the absence of any zinc enrichment in control sample CCBS:17, this having similar values to those detected in CCBS:13 to CCBS:15.

PARTICLE SIZE DISTRIBUTION (PSD)

Sieve analysis provided PSD by weight for the Croig Cave bulk samples (Table 12), with descriptions in terms of texture, sorting and modality provided in Table 13. The quantities of bulk material from each sample measured by sieve analysis were variable. All were in excess of 1,400g, with the exception of CCBS:6 and CCBS:7 that provided 334.4g and 744.7g respectively.

PSD determinations indicated that the sediment matrix throughout the midden is comprised of poorly to very poorly sorted gravels, ranging from very fine to coarse, with CCBS:6, CCBS:12 to CCBS:13 and CCBS:15 containing a mix of gravels with

TABLE 13
Classification of sediments according to modality, sorting and texture

Bulk sample	*Sample type*	*Degree of sorting*	*Texture*
PHASE 3: HISTORIC			
CCBS:1	Unimodal	Poorly sorted	Medium gravel
CCBS:2	Trimodal	Poorly sorted	Very coarse gravel
CCBS:3	Bimodal	Poorly sorted	Medium gravel
PHASE 2: IRON AGE			
CCBS:4	Bimodal	Poorly sorted	Coarse gravel
CCBS:5	Bimodal	Poorly sorted	Very fine gravel
CCBS:6	Unimodal	Poorly sorted	Sandy very fine gravel
CCBS:7	Trimodal	Poorly sorted	Very fine gravel
CCBS:8	Bimodal	Poorly sorted	Very fine gravel
CCBS:9	Bimodal	Poorly sorted	Very fine gravel
CCBS:10	Bimodal	Poorly sorted	Medium gravel
PHASE 1: BRONZE AGE			
CCBS:11	Bimodal	Poorly sorted	Very fine gravel
CCBS:12	Unimodal	Poorly sorted	Sandy very fine gravel
CCBS:13	Bimodal	Poorly sorted	Sandy fine gravel
CCBS:14	Unimodal	Poorly sorted	Medium gravel
CCBS:15	Bimodal	Poorly sorted	Sandy fine gravel
CCBS:16	Trimodal	Very poorly sorted	Very coarse gravel

sand-sized particles. Most samples were multi-modal with the exception of CCBS:1, CCBS:6, CCBS:12 and CCBS:14 falling within the unimodal type.

LOSS ON IGNITION (LOI)

Table 9 incorporates LOI measurements providing weight percent proportions of organic material lost through ignition, illus 13. LOI values range from a minimum of 3.35% in CCBS:11 to a maximum of 4.37% in CCBS:9. Overall, the standard deviation of LOI values is low at 0.3, based on an average of 3.7%. This indicates that the data points tend to be very close to the mean, though the highest values tend to occur in the levels above CCBS:14, corresponding with the levels where molluscs and charcoal were most abundant. Both control samples produced LOI values within the range obtained from the midden samples, lending support to the suggestion that its composition is likely to consist of both cave and beach sediments.

MAGNETIC SUSCEPTIBILITY

Mass specific magnetic susceptibility results are provided in Table 14 and illus 13. The magnetic susceptibility values of 14.23 SI (CCBS:17) and 14.42 SI (CCBS:18) obtained from the control samples are similar to those from soils over diabase rock as determined by Tite (1972). Diabase is a mafic, holocrystalline, subvolcanic rock equivalent to volcanic basalt found extensively on Mull.

Magnetic susceptibility of samples in levels above CCBS:15 exhibit considerable enhancements with respect to the 'background' values obtained from the controls, with the exception of CCBS:13 that provided a minimum value of 12.34 SI. Illus 13 shows magnetic susceptibility values increasing in successive levels above CCBS:12, with the greatest enhancement indicated in CCBS:1 to CCBS:5, CCBS:7 and CCBS:9 with values ranging from 46.87–74.74 SI. The magnetic susceptibility of soils and sediments can be enhanced by burning as it transforms

TABLE 14
Magnetic susceptibility of matrix sediments

Bulk sample	*Mass Specific Magnetic Susceptibility (SI)*
PHASE 3: HISTORIC	
CCBS:1	46.87
CCBS:2	68.87
CCBS:3	73.42
PHASE 2: IRON AGE	
CCBS:4	71.22
CCBS:5	74.74
CCBS:6	40.09
CCBS:7	60.60
CCBS:8	41.56
CCBS:9	64.28
CCBS:10	43.20
PHASE 1: BRONZE AGE	
CCBS:11	40.04
CCBS:12	17.39
CCBS:13	12.34
CCBS:14	22.04
CCBS:15	14.57
CCBS:16	14.66
CONTROL SAMPLES	
CCBS:17	14.42
CCBS:18	14.23

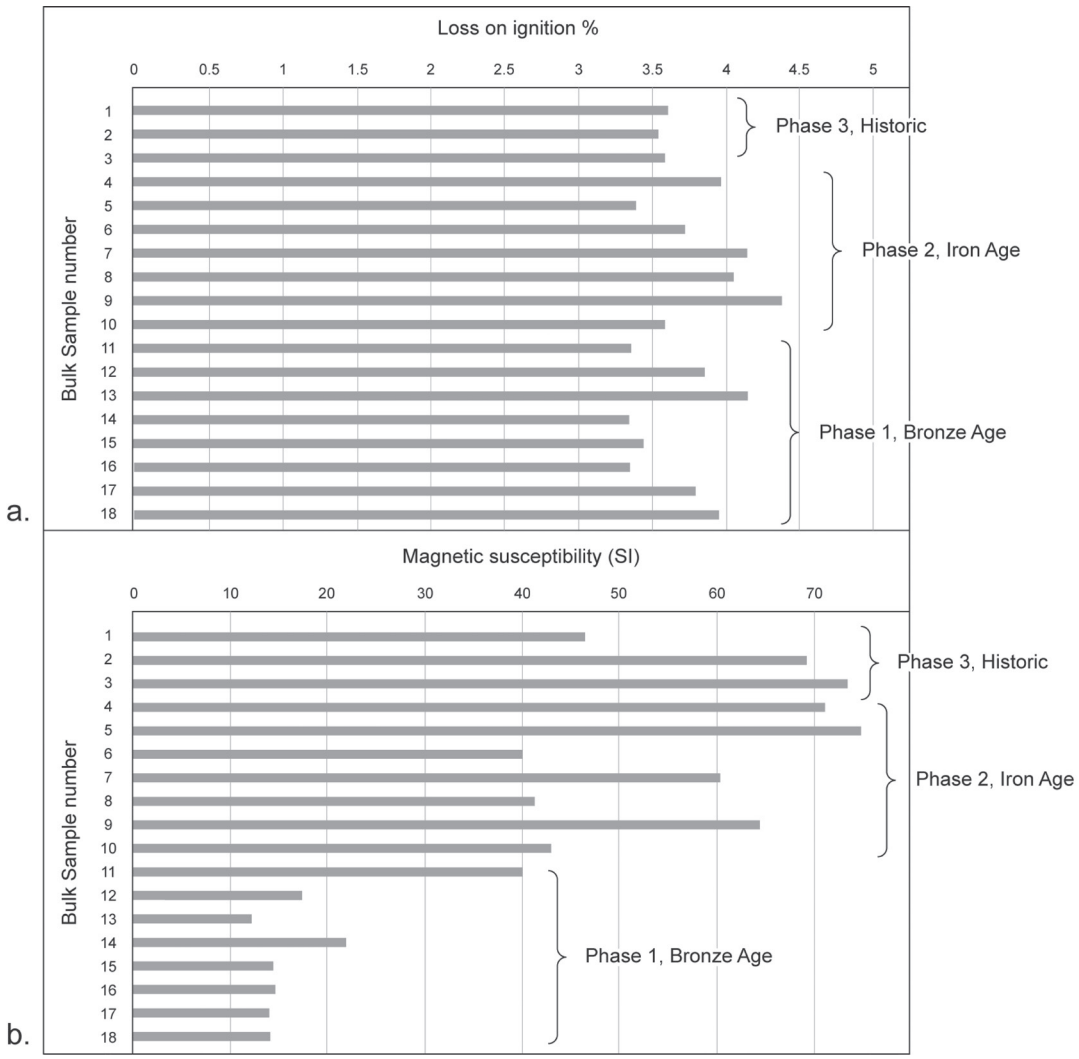

ILLUS 13 Chart showing (a) loss on ignition and (b) mass specific magnetic susceptibility of matrix sediments, Croig Cave

weakly magnetic forms of iron oxide (hematite) into strongly ferromagnetic crystalline forms (maghaemite) (Longworth & Tite 1977). In light of the quantities of charcoal and zinc in the levels above CCBS:10, it is likely that such magnetic enhancement of iron oxides has occurred. This indicates that these levels contain significant quantities of burnt in situ sediments.

MIDDEN ANALYSIS

FISH BONES

Claire Ingrem

The analysed fish assemblage consists of 14,338 fragments, of which 11% is identifiable. Eighty-two per cent of this assemblage was retrieved using 2mm and 1mm mesh sieves.

TABLE 15
Quantities, fragmentation, condition and size of fish bones

Bulk sample no of fish bones (bones/gm sediment)	*Description*	*Condition, % of identifiable assemblage*	*Fragmentation, % of identifiable assemblage*	*Surface modification % of identifiable assemblage*	*Fish estimated (NISP)*
	PHASE 3: HISTORIC				
CCBS:1 3802 (0.99)	This sample has highest density of fish bone. Like the other samples, it is dominated by butterfish – although it differs in respect of the abundance of whiting (Table 16) and the fact that a smaller proportion of bone is in good condition. Eel (*Anguilla anguilla*) and bullrout (*Myoxocephalus scorpius*) are the most numerous of the other taxa, most of which are represented by just a few bones each. Vertebral bones dominate the material although some cranial bones are again present, particularly those belonging to whiting (*Merlangius merlangus*) and bullrout.	Good 79 Medium 21 Poor <1	100%: 1 75–100%: 58 50–75%: 18 25–50%: 10 <25%: 13	Crushed: 0 Burnt: 1	Large: 0 Medium: 7 Small: 192 Very small: 197
CCBS:2 413 (0.18)	This is relatively poor in fish bones compared with the samples taken from above and below although a range of similar taxa are represented by a few bones, with butterfish *(Pholis gunnellus)* the most numerous. Wrasse (*Labridae*) is the only taxa represented by cranial bones – a dentary and a hyomandibular.	Good 100 Medium 0 Poor 0	100%: 0 75–100%: 59 50–75%: 22 25–50%: 3 <25%: 16	Crushed: <1 Burnt: 4	Large: 0 Medium: 1 Small: 16 Very small: 15
CCBS:3 1143 (0.16)	Butterfish continue to be the most numerous species with eel, wrasse and sea scorpion relatively well represented. Several bones belong to sand eel (Ammodytidae) although, being caudal vertebrae, they could well derive from a single individual. The assemblage is once again dominated by vertebra although with the exception of eel, cranial bones belonging to the major taxa are again present, particularly in respect of wrasse.	Good 97 Medium 3 Poor 0	100%: 3 75–100%: 68 50–75%: 14 25–50%: 12 <25%: 5	Crushed: 0 Burnt: 2	Large: 0 Medium: 6 Small: 50 Very small: 98

Bulk sample no of fish bones (bones/gm sediment)	*Description*	*Condition, % of identifiable assemblage*	*Fragmentation, % of identifiable assemblage*	*Surface modification % of identifiable assemblage*	*Fish estimated (NISP)*
		PHASE 2: IRON AGE			
CCBS:4 2479 (0.49)	This is the second richest sample in the whole assemblage. Eel, rockling (Lotidae), wrasse and scorpion fish (Scorpaenidae) are all quite numerous and a variety of gadoids (Gadidae) are represented, although bones belonging to butterfish continue to dominate, comprising more than a quarter of the assemblage (Table 16). As in previous samples, the assemblage is dominated by vertebrae although some cranial bones are present, particularly those belonging to wrasse.	Good 96 Medium 4 Poor <1	100%: 1 75–100%: 60 50–75%: 17 25–50%: 11 <25%: 11	Crushed: <1 Burnt: <1	Large: 0 Medium: 2 Small: 170 Very small: 214
CCBS:5 474 (0.11)	In addition to the usual predominance of butterfish and wrasse, hake (Gadidae) are quite numerous. This sample contains the second highest proportion of burnt bone.	Good 93 Medium 5 Poor 1	100%: 1 75–100%: 45 50–75%: 16 25–50%: 19 <25%: 19	Crushed: 1 Burnt: 7	Large: 0 Medium: 2 Small: 36 Very small: 37
CCBS:6 183 (0.05)	A sample with relatively few fish remains, although again, wrasse and butterfish are the most numerous taxa (Table 16).	Good 94 Medium 6 Poor 0	100%: 0 75–100%: 55 50–75%: 18 25–50%: 18 <25%: 9	Crushed: 1 Burnt: 4	Large: 0 Medium: 0 Small: 26 Very small: 7
CCBS:7 123 (0.03)	This is the poorest sample in terms of fish bone with just thirteen identifiable fragments present in the sub-sample examined, three of which belong to butterfish.	Good 100 Medium 0 Poor 0	100%: 0 75–100%: 53 50–75%: 18 25–50%: 18 <25%: 12	Crushed: 1 Burnt: 4	Large: 0 Medium: 2 Small: 9 Very small: 6

Bulk sample no of fish bones (bones/gm sediment)	*Description*	*Condition, % of identifiable assemblage*	*Fragmentation, % of identifiable assemblage*	*Surface modification % of identifiable assemblage*	*Fish estimated (NISP)*
CCBS:8	The only taxa that is well represented is butterfish, although several bones belonging to wrasse and sea scorpion are also present (Table 16).	Good 97 Medium 3 Poor 0	100%: 1 75–100%: 49 50–75%: 26 25–50%: 9 <25%: 15	Crushed: 0 Burnt: 10	Large: 0 Medium: 2 Small: 25 Very small: 41
CCBS:9 580 (0.11)	This sample is rich in fish bone with butterfish the most numerous species. Once again, a variety of other fish are represented, but all by just a few bones (Table 16).	Good 98 Medium 2 Poor 0	100%: 0 75–100%: 52 50–75%: 19 25–50%: 12 <25%: 17	Crushed: 1 Burnt: 5	Large: 1 Medium: 7 Small: 43 Very small: 48
CCBS:10 844 (0.13)	In respect of density and taxa representation, this sample is very similar to sample 14 (Table 16), being dominated by butterfish with gadoid fish (particularly rockling), wrasse and sea scorpion relatively well represented compared to the wide range of taxa that, once again, are present in small numbers. The sample clearly displays a similar pattern to that observed in earlier deposits, being dominated by vertebrae but with the major taxa also represented by a few cranial bones, especially wrasse.	Good 99 Medium 1 Poor 0	100%: 0 75–100%: 49 50–75%: 20 25–50%: 17 <25%: 14	Crushed: <1 Burnt: 2	Large: 0 Medium: 10 Small: 58 Very small: 106
	PHASE 1: BRONZE AGE				
CCBS:11	This sample is rich in fish bone. As with previous samples, a range of taxa are represented although butterfish are more than twice as numerous as any other taxa, apart from sea scorpion. Pipefish (Syngnathidae), whiting, other small gadoid fish and wrasse (probably corkwing, *Crenilabrus melops*) are also relatively numerous (Table 16). Once again, the assemblage is dominated by vertebrae, although cranial bones belonging to gadoid fish are quite numerous; wrasse and sea scorpion are also fairly well represented by bones from the head.	Good 98 Medium 2 Poor <1	100%: <1 75–100%: 58 50–75%: 15 25–50%: 10 <25%: 17	Crushed: 1 Burnt: 3	Large: 0 Medium: 5 Small: 83 Very small: 129

Bulk sample no of fish bones (bones/gm sediment)	*Description*	*Condition, % of identifiable assemblage*	*Fragmentation, % of identifiable assemblage*	*Surface modification % of identifiable assemblage*	*Fish estimated (NISP)*
CCBS:12 532 (0.09)	The few specimens within this sample belong to a range of taxa with wrasse and sea scorpion the most numerous species, both of which are represented by both cranial and vertebral bones (Table 16).	Good 96 Medium 4 Poor 0	100%: 0 75–100%: 51 50–75%: 16 25–50%: 20 <25%: 13	Crushed: 1 Burnt: 1	Large: 0 Medium: 2 Small: 20 Very small: 33
CCBS:13 525 (0.07)	This sample contained a similar density of fishbone to sample 30 and also a wide range of taxa. More than half of the identifiable bones belong to rockling, wrasse and butterfish (Table 16).	Good 99 Medium 1 Poor 0	100%: 2 75–100%: 47 50–75%: 13 25–50%: 16 <25%: 22	Crushed: <1 Burnt: 2	Large: 0 Medium: 0 Small: 59 Very small: 48
CCBS:14 807 (0.12)	A wide range of taxa are present in this sample, although most are represented by just a few specimens; rockling, wrasse, butterfish and sea scorpion are relatively well represented. The assemblage is dominated by vertebrae, although cranial bones belonging to eel, wrasse and sea scorpion are also present.	Good 99 Medium 1 Poor 0	100%: 1 75–100%: 54 50–75%: 19 25–50%: 11 <25%: 16	Crushed: <1 Burnt: 1	Large: 0 Medium: 3 Small: 87 Very small: 93
CCBS:15 521 (0.08)	This sample contained a wide range of taxa with none particularly numerous (Table 16): members of the salmon family (Salmonidae), European hake (*Merluccius merluccius*), dragonet (*Callionymus lyra*), bullrout, sea scorpion and stickleback (Gasterosteidae) are present. Wrasse bones, including corkwing (*Crenilabrus melops*), are quite numerous. The majority of the bones are again vertebrae, although some cranial bones belonging to whiting, rockling, corkwing, and sea scorpion are also present.	Good 99 Medium 1 Poor 0	100%: 0 75–100%: 40 50–75%: 17 25–50%: 21	Crushed: <1 Burnt: <1	Large: 0 Medium: 0 Small: 53 Very small: 46

Bulk sample no of fish bones (bones/gm sediment)	*Description*	*Condition, % of identifiable assemblage*	*Fragmentation, % of identifiable assemblage*	*Surface modification % of identifiable assemblage*	*Fish estimated (NISP)*
CCBS:16 199 (0.04)	This sample is relatively poor in fish bones and consequently only 24 identifiable specimens were examined. However, a range of taxa are represented including eel, conger eel (*Conger conger*), great pipefish (*Syngnathus acus*), whiting, greater forkbeard (*Phycis blennoides*), rockling, wrasse, butterfish, bullrout, hook-nose (*Agonus cataphractus*), dab (*Limanda limanda*) and sole (Soleidae), but none are particularly frequent. The sample is too small to provide meaningful information concerning body part representation, although in addition to vertebra, a few cranial bones belonging to gadoid fish, dab and sole are present.	Good 91 Medium 9 Poor 0	100% : 0 75–100%: 46 50–75%: 20 25–50%: 17 <25%: 17	Crushed: <1 Burnt: <1	Large: 0 Medium: 0 Small: 12 Very small: 23

The majority of the bones are in good condition; more than 75% of the bones are complete and evidence of burning and gnawing (in the form of crushing) are scarce. Almost all of the bones belong to small or very small fish. Table 15 summarises the bone assemblage from each of the 16 samples, while Table 16 lists the species identified within each sample.

A wide range of taxa are present – although only common eel (*Anguilla anguilla*), butterfish (*Pholis gunnellus*) and sea scorpion (*Taurulus bubalis*) comprise more than 5% of the identifiable assemblage. Cod family (Gadidae) and wrasse (Labridae) also constitute more than 5% of the assemblage with most of the remains assigned to the latter probably derived from corkwing (*Crenilabrus melops*).

The largest quantity of fish bones came from the Saple CCBS:1, although CCBS:3 and CCBS:4 also produced relatively large assemblages (illus 14a). Other large samples, including CCBS:10, CCBS:11 and CCBS:14, came from the middle and lower half of the midden. The most striking characteristic of the assemblage is the abundance of bones belonging to small and very small fish, many of which have no economic value today; almost as striking is the similarity in the composition of the fish assemblage from each of the 16 bulk samples. The number of species within each bulk sample correlates with the number of bones, reaching an asymptote of 32 species at between 1,500–2,000 bones (illus 15a).

All the major taxa – and most of the trace taxa – are commonly found in rock pools and on the sea shore. Eels are common in rivers, estuaries and the European seaboard; according to Wheeler (1967: 227), those found in the sea and estuaries are generally small, bury themselves in muddy and sandy bottoms, and are very common where suitable pools exist between the tide marks. Butterfish are also common on the sea shore, where they generally inhabit the area between the mid to low tide levels and are found under rocks and in crevices. Sea scorpion are common on all rocky ground where there

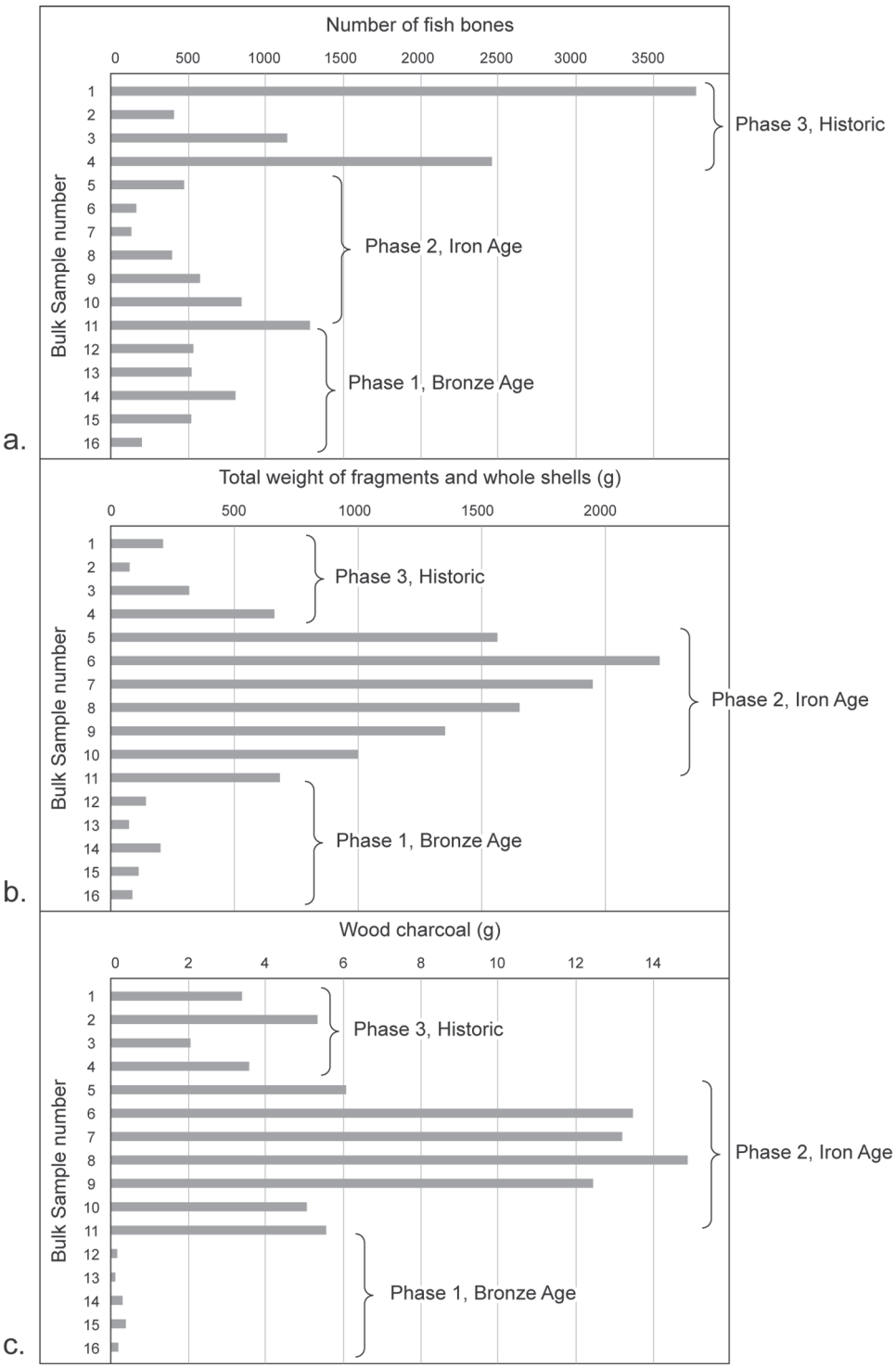

ILLUS 14 Chart showing (a) number of fish bones, (b) total weight of mollusc shell, and (c) total weight of wood charcoal, for each bulk sample

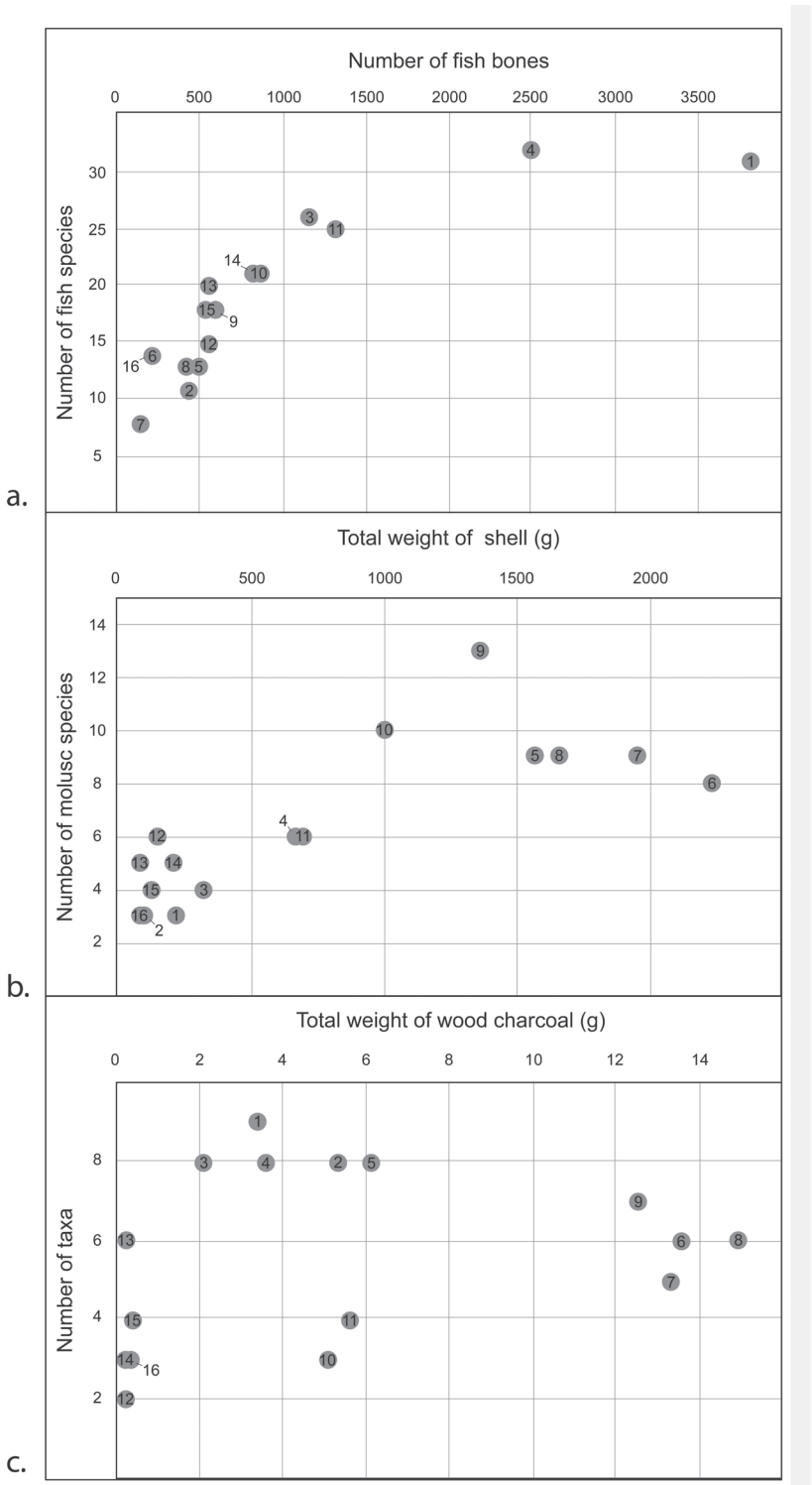

ILLUS 15 The relationship between species/taxa frequency and sample size for (a) fish bones, (b) mollusc shell, and (c) wood charcoal

is a covering of seaweed, whilst the closely related bull rout is found on sandy and muddy bottoms and in estuaries. Wrasses too, are found in shallow water, particularly corkwing which is known to be an abundant resident of rocky shore pools (Wheeler 1967).

Immature gadoid fish are also commonly found close inshore, particularly species such as whiting (*Merlangius merlangus*) and bib (*Trisopterus luscus*) which inhabit shallow sandy waters, and rockling. Shore rockling (*Gaidropsarus mediterraneus*), as the name suggests, inhabit the shore where they live in rock pools and under algae. Five-bearded rockling (*Ciliata mustela*) is abundant between tide marks on rocky shores and in intertidal pools on sand, where protection is afforded by loose boulders. Most of the other minor taxa are also known to inhabit the inshore zone and many, such as pipefish (*Syngnathinae*) and dragonet (*Callionymidae*), are commonly found in rock pools; young flatfish are similarly common in shallow water, soles are often found on sandy or muddy ground (ibid).

The small size of the fish and the range of taxa present suggested initially that the assemblage might not have an anthropogenic origin. Otters (*Lutra lutra*) commonly eat small fish between 50mm and 150mm – such as butterfish, sea scorpion and sand eel (Watt 1992) – and collections of fish bones resulting from otter activity are sometimes found at archaeological sites (Ceron-Carrasco 1998; 1999; 2003). Such evidence generally occurs in confined areas which would have made suitable holts, although it can occur outside entrances to dens because once weaned, the young defecate outside (Chanin 1988). In the present day, otter holts can be found in the vicinity of Croig Cave and so it would not be surprising if they inhabited the area during the period in which the midden accumulated. However, there is little evidence for chewing and digestion, which are major characteristics of otter accumulated assemblages (Céron-Carrasco 1998; 1999; 2003), and the excavation did not provide evidence for burrowing. In addition, the fish bones were thoroughly intermixed with material of unquestioned anthropogenic origin and, as sprainting is used for social communication, otters are unlikely to have used a shell midden while it was also in use by humans (Jan Watt pers comm) since any spraints would soon become covered with shell.

The remains of very small fish often occur in small numbers in assemblages consisting predominantly of bones belonging to larger fish and, in this situation, are usually interpreted as gut contents. However, bones belonging to large and even medium-size fish are scarce at Croig Cave which suggests that, unless other food waste was disposed of separately, this type of explanation is unlikely. The overall scarcity of mammal bones in the midden suggests that it was used mainly for disposing of waste associated with processing resources collected on the sea shore. Consequently, it is possible that large fish were gutted at Croig Cave and then transported elsewhere to be cooked and eaten. However, evidence for offshore fishing involving the capture of substantial numbers of large fish is not generally seen until the Norse period and so this explanation appears unlikely for the Bronze and Iron Age phases of the midden.

Humans have exploited small fish for food throughout history. According to Cutting (1956: 16), travellers accounts from Africa suggest that none were considered too small, with fish the size of minnows sun-dried whole and, although pungent, used to flavour cereal dishes. Even the Romans are known to have valued small fish with which they used to make a sauce known as *garum* (Bateman & Locker 1982). In the present day, small eels and particularly immature elvers (Schweid 2002) are considered a culinary delicacy and small (25–50mm) clupeids are commonly eaten as whitebait in Britain.

Watt (1995) has shown that a similar range of taxa can be caught on the coast of Mull with unbaited traps set near the lower edge of the intertidal zone and this is likely to have been the case in the past. Indeed, it would be surprising

if edible resources offered by rock pools on the sea shore were not exploited by humans during the prehistoric period. Minimal technology would have been required, fish being scooped up in nets, baskets or hands after having been trapped in shallow pools. Ethnographic sources concerning later populations living in the Northern Isles of Scotland, suggest that the collection of shellfish and other shore resources was carried out on the community scale in order to minimise the time taken in searching for resources that were patchily distributed (Anderson 1981; Colley 1983). Consequently, it is unlikely that this type of activity would have been focused on any single resource: all the edible fish and shellfish that were encountered would have been collected. On Orkney, collecting small fish, such as five-bearded rockling and bull rout, from shore pools and from amongst seaweed was a simple type of fishing practised by the inhabitants (Colley 1983). In an ethnographic study of Orkney and Shetland, Fenton (1978: 542) mentions that shore resources 'often formed part of the food of the poor'. Little risk would have been involved in this type of strategy but as it would only have offered a low calorific return, the main aim may have been simply to add variety to the diet (Colley 1983).

The predominance of vertebrae is not unexpected, given their abundance in the skeleton compared with other elements, their relative robustness and relative ease in which they can be identified. However, the presence of whole fish is attested by the survival of some cranial bones belonging to many of the taxa present. The relatively high incidence of head bones from wrasse is probably partly due to the recovery of several pharyngeal bones, which are particularly distinctive and robust. It is likely that, in general, body part representation has been severely biased by bone density in light of the relatively high incidence of jaw bones compared to thinner, more fragile skull bones.

It is perhaps surprising to find so many small bones given the current practice of eating small fish, such as whitebait, whole. Whitebait are approximately 4–5cm in length and this is considerably smaller than most of the fish recovered from Croig Cave. Comparison with reference material suggests that the smallest Croig fish were at least twice, if not three times, the size of modern day whitebait and consequently their bones may well have been unpalatable. The likelihood that small fish caught on the shore required some preparation prior to consumption is also suggested by the presence of bull rout whose head spines can cause septic wounds, and hook-nose which is covered in hard bony plates that form rows of sharp spines.

Discussion

Bronze Age sites which have produced assemblages of fish bone are scarce in the Hebrides. However, low risk exploitation of the inshore zone is a feature of prehistoric assemblages from both the Western and Northern Isles of Scotland, most of which are dominated by small gadoid fish (Colley 1983; Cerón-Carrasco 1999; Ingrem 2000). Evidence for exploitation of the immediate environment during the Mesolithic period comes from a few sites including Fiskary Bay, located immediately opposite Croig Cave on the coast of Coll (Steven Mithen pers comm). The small assemblage that was recovered from Fiskary Bay was similarly composed mainly of bones belonging to small, inshore fish, most of which occur in the Croig samples. A Mesolithic site on Oronsay produced an assemblage dominated by young saithe (*Pollachius virens*), believed to have been caught at several different times of the year (Mellars & Wilkinson 1980). The only large assemblage of Bronze Age fish bones to come from the Western Isles was recovered from Cladh Hallan on South Uist and this is similarly dominated by immature saithe (Ingrem forthcoming a). Beaker deposits at Rosinish on Benbecula produced only two identifiable

TABLE 16
Identifiable fish bones

	Phase 3: Historic			*Phase 2: Iron Age*							*Phase 1: Bronze Age*						*Total*
Bulk sample, CCBS:	1	2	3	4	5	6	7	8	9	10	11	12	13	14	15	16	
Clupea harengus				1													1
Clupeidae spp														1			1
Coregonidae spp							1										1
Salmonidae spp	4		2	6				1		5	2	1	1	3	1		26
Anguilla anguilla	26	2	9	19	2	1		2	1	10	7	3	6	7	4	1	100
cf *anguilla anguilla*														1			1
Conger conger	2	1		4	2			1	3	3	3	2	2	4	1	1	29
Syngnathus acus		1	2	1	2			1	1	2	13	1	1	2	3	2	32
cf *syngnathidae* spp			1														1
Gadidae spp	37		4	25	4	3	1	5	5	5	16	6	2	7		3	123
cf *gadidae* spp	2			2				3		2	1		1	4			15
Micromesistius poutassou			1														1
Merlangius merlangus	49	4	2	1		1		1			13			1	2	1	75
cf *merlangius merlangus*	4										1						5
Trisopterus spp	3		2	1						2		1					8
cf *trisopterus* spp		1															2
Trisopterus luscus		1					1										2
Trisopterus minutus				3													3
Pollachius pollachius	1			2							1						4
Pollachius virens	5		4	3	3						4		1	4			24
Gadus morhua	2	1		2	2		3	2			3						15
Phycis blennoides			3	6					2				2		1	1	15

	Phase 3: Historic			*Phase 2: Iron Age*							*Phase 1: Bronze Age*						*Total*
Merluccius merluccius		1		7	7	2				9		1	1	1	5		34
Volva molva						1											1
Gaidropsarus mediterraneus			3	18					2								23
Gaidropsarus vulgaris												1			1		2
Rhinonemus cimbrius	1								7	7	6	1		1			23
Ciliata mustela	8		5	10		1	1	1		3	1		10	11	4	3	58
Gaidropsarus/Rhinonemus/ Ciliata spp	6		3	10				1	3	2	5	3	3	3	2	2	43
Dicentrarchus labrax	6			4													10
cf *dicentrachus labrax*				1													1
Trachurus trachurus	1		3				1			2							8
Spondyliosoma cantharus	7																7
Labridae spp	10	3	13	17	7	1		4	3	15	13	5	9	13	9	2	125
cf *labridae* spp			2				1	2	2	3					2		12
Crenilabrus melops	1		1	8	3	4			2	2	3	2	1	2	3		34
Labrus bergylta	4		1		1				2		1		2				13
Ammodytes spp	1		7			1								3			13
cf *gobidae* spp													1		1		2
cf *callionymidae* spp	1										1						2
Callionymus lyra	4			8	3			1	1		1	2	2	3	2		27
Pholis gunnellus	75	8	36	84	10	4	3	19	25	25	28	3	19	29	5	2	375
cf *pholis gunnellus*	1	2	2	2						1	1					1	10
Sebastes viviparus				3													3
Triglidae spp	6			2										4			12
cf *triglidae* spp	1																1

	Phase 3: Historic			*Phase 2: Iron Age*							*Phase 1: Bronze Age*						*Total*
Cottidae spp	3		1	2		1		2		1			1	4	2		17
cf *cottidae* spp				1	1					1				2	2		7
Myoxocephalus scorpius	23		5	1		2				3	2	2	1	2	1	1	44
cf *myoxocephalus scorpius*	2			2													4
Taurulus bubalis	1		8	35	4		1	6	5	15	21	5	5	17	2		125
cf *taurulus bubalis*			2	3												1	6
Agonus cataphractus			1	1					1	1	5				1	1	11
cf *agonus cataphractus*															1		1
Gasterosteidae spp	1																1
Scophthalmus maximus						1											1
Scophthalmus rhombus										1							1
Pleuronectidae spp	10	1		3		1			1	2	2			5			25
Limanda limanda	1		1						2		1		1			1	7
cf *limanda limanda*				2													2
Platichthys flesus											2						2
Pleuronectes platessa	1		1	2					1								5
Microstomus kitt				1													1
Soleidae spp																1	1
Flatfish	1		2	2					1	1	1			1			9
cf *flatfish*	1		1					1	1	1	1						6
Unidentifiable	3489	388	1015	2174	423	159	110	345	509	720	1136	493	462	673	466	175	12739
Total	3802	415	1143	2479	474	183	123	398	580	844	1295	532	535	807	521	199	14338
Total identifiable	312	26	128	305	51	24	13	53	71	124	159	39	73	134	55	24	1599
% identifiable	8	6	11	12	11	13	11	13	12	15	12	7	14	17	11	12	11

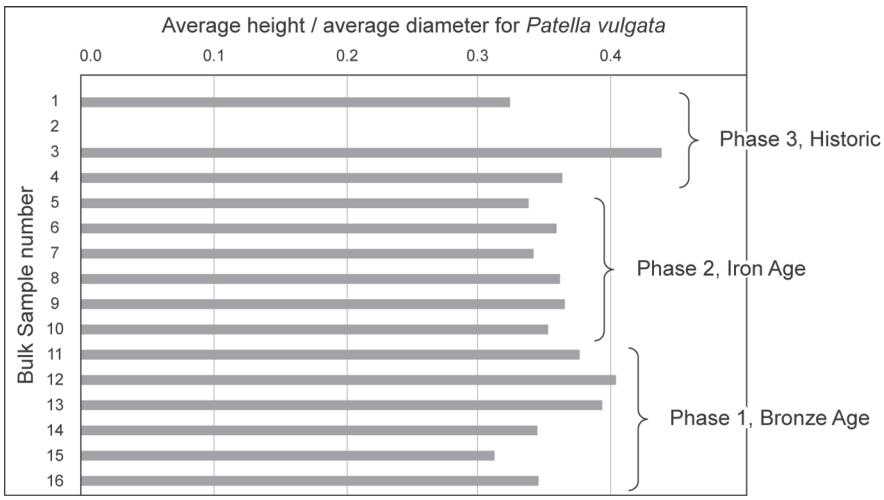

ILLUS 16 Height/diameter (averages) of limpet (*Patella vulgata*) for each bulk sample

fish bones, but both belong to cod family fish (Dale Serjeantson pers comm). A low risk strategy was also practised during the Iron Age as indicated by deposits on Sandray (Ingrem 2000), Mingulay (ibid), and South Uist (Cerón-Carrasco 1999; Ingrem forthcoming b). In contrast, there is evidence to suggest that higher risks were taken during the Norse period, with many sites dominated by herring and large cod and hake family fish indicating that offshore waters were being exploited (Ingrem 2005: 157; Ingrem forthcoming c). At Croig Cave, there is nothing to suggest that offshore waters were exploited during the historic period, although whiting, which is a good eating fish, may have been preferentially selected.

The assemblage of fish bones recovered from Croig Cave strongly suggests that small fish were caught in rock pools and shallow inshore waters. Many of the taxa recovered from Croig Cave are often associated with otter activity but contextual evidence suggests that here, this is unlikely. It is also unlikely that the remains derive from the gut contents of larger fish since there is little evidence to suggest that larger fish were exploited during the Bronze Age. There is plentiful evidence, both ethnographic and archaeological, to suggest that throughout history small fish were eaten and even today, some are considered culinary delicacies. Most prehistoric assemblages from the Northern and Western Isles of Scotland are dominated by small cod family fish, particularly saithe, indicating that a low risk strategy involving the exploitation of inshore waters was usual at this time. At Croig Cave, it appears that a low risk strategy was also employed but was focused on more varied resources.

MAMMAL, BIRD AND AMPHIBIAN BONES

Claire Ingrem

A small number of non-fish bones were acquired from the bulk samples (Table 17) including those of rodents (n=21), amphibians (n=15), birds (n=2), red deer (*Cervus elaphus*) (n=1) and unidentifiable small and medium mammal bones (n=8). These primarily came from the higher levels within the sequence, the highest number (n=11) coming from CCBS:2. There is no reason why any of these animal bones should necessarily derive from human activity:

rodents, birds and amphibians may have been living in the cave or represent the remnants of carnivore activity, as might the mammal bones. Alternatively, all of these species, with the exception of the rodents, might reflect a further element of human foraging activity.

Larger non-fish bones were also hand-picked from deposits during excavation and recorded by context (Table 18). These were few in number and covered a similar range of animal types, with the addition of domesticated species – cattle (*Bos* sp), sheep/goat (ovicaprids) and pig (*Sus* sp). The cattle and pig bones were restricted to the three most recent contexts (CC101, CC102 and CC103), along with five of the six sheep/goat bones. The only other notable find is a single bone from the Great Auk (*Pinguinus impennis*) from CC101.

MOLLUSCS

Sarah Elliott

A total of 12,377g of mollusc shell was recovered, within which 17 species of gastropods and bivalves were identified. The assemblage as a whole was dominated by common limpet (*Patella vulgata*; 61.18%) with the next most common species being the common periwinkle (*Littorina littorea*) and rough periwinkle (*Littorina saxatilis*; 35% combined) (Tables 19 and 20).

The concentration of mollusc shell showed considerable variation through the sequence (illus 14b), with high densities in the central part of the sequence. These samples also have the highest frequency of species (illus 15b). Limpet is the most frequent species in all samples other than CCBS:5, CCBS:11, CCBS:10 and CCBS:15 which are dominated by periwinkles.

All the samples from Croig Cave are dominated by edible marine molluscs. Limpets live on rocks or stones from high shore down to the edge of the sub-littoral zone; they are mobile, live on algae and are found on all British coasts. Periwinkles are also abundant on all British coasts on rocky shores (Graham 1988). They prefer sheltered locations and are not often found in exposed areas. The periwinkle *saxatalis* group can be found mainly on the upper rocky shores amongst weeds. Other marine species such as razor clam (*Ensis* spp) and blue mussel (*Mytilus edulis*) are also edible. Razor clams are commonly found burrowed into sand, while blue mussels can be found in a wide range of coastal habitats, particularly open coasts with rocky shores. Three species of land snails were found in small quantities in some of the samples: the waxy glass snail (*Aegopinella nitidula*), the common chrysalis snail (*Lauria cylindracea*) and the rotund disc (*Discus rotundatus*). These were probably living in the cave and are indicative of a sheltered rocky environment.

The centre of the sequence, between CCBS:4 and CCBS:10, is the period of intensive use of the cave, with a peak represented by CCBS:6 and CCBS:7. A dominance of limpets over periwinkles was recorded in CCBS:6 to CCBS:9, whereas CCBS:11 and CCBS:10 show the reverse.

Measurements of molluscs within shell middens can be informative about collecting strategies: squat limpets tend to come from mid or low shore while limpets with a pronounced cone tend to come from the upper shore (Classen 1998). Illustration 16 shows the average height:diameter ratio for whole limpets within each of the sixteen samples (992 limpets; using average values for each sample). This shows limited variation throughout the sequence, suggesting either a long-term preference for collecting a certain size of limpet or a consistent size distribution of molluscs within the vicinity of the cave and a random collecting strategy. The former seems most likely because the size distribution is generally fairly large in comparison to the University of Reading reference collection, which represents limpets from throughout Britain. The same pattern is present for both species of periwinkle. In light of the consistency of size throughout

TABLE 17
Mammal, bird and amphibian bones recovered by wet sieving

Bulk sample (total non-fish bones)	*Sheep/ goat*	*Red deer*	*Field Vole*	*Vole*	*Rodent mammal*	*Medium mammal*	*Small*	*Thrush*	*Bird*	*Amphibian*
PHASE 3: HISTORIC										
CCBS:1 (1)										1
CCBS:2 (11)			1 (mandible)	1	4	4		1 (tarsmeta-tarusus)		
CCBS:3 (3)				1	1				1 (tarsmeta-tarusus)	
PHASE 2: IRON AGE										
CCBS:4 (9)		1 (metatarsal)		1	2		1 (vertebrae)			4
CCBS:5 (6)					3 (incisor, humerus, radio-ulna)		1 (caudal vertebrae)			2 (vertebra)
CCBS:6 (3)				2 (mandible, molar)	1					
CCBS:7 (1)					1 (scapula)					
CCBS:8 (2)					1 (tibia)	1 (rib fragment)				

Bulk sample (total non-fish bones)	*Sheep/ goat*	*Red deer*	*Field Vole*	*Vole*	*Rodent mammal*	*Medium mammal*	*Small*	*Thrush*	*Bird*	*Amphibian*
CCBS:9 (5)	.				1 (incisor)	2 (rib fragments)	1 (lumbar vertebrae)			1 (femur)
CCBS:10 (5)						2	1			2 (limb bones)
PHASE 1: BRONZE AGE										
CCBS:11 (5)						1 (caprine metacarpal)	1 (caudal vertebrae)			2 (limb bones)
CCBS:12 (1)										1 (limb bone)
CCBS:13 (0)										
CCBS:14 (2)					1 (femur)					1 (femur)
CCBS:15 (0)										
CCBS:16 (1)										1

TABLE 18
Bones by context, hand-picked from contexts

	Cattle	*Sheep*	*Sheep/ goat*	*Pig*	*Red deer*	*Large mammal*	*Medium mammal*	*Small mammal*	*Vole*	*Rodent*	*Great auk*	*Thrush*	*Amphibian*	*Total*
PHASE 3: HISTORIC														
CC101	2	2		1	1	1	9	2	1	1	1		1	22
CC102	2		3			3	4					1	1	14
PHASE 2: IRON AGE														
CC103	2			2	3	8	3							18
PHASE 1: BRONZE AGE														
CC104					1									1
CC109			1			1								2
Total	6	2	4	3	5	13	16	2	1	1	1	1	2	57

TABLE 19
Presence of identifiable molluscs

	Patella vulgata	*Patella Pellucida*	*Littorina littorea*	*Littorina* 'saxatalis group'	*Littorina littoralis*	cf *Lacuna crassior*	*Cepaea nemoralis*	*Cepaea* spp	cf *Gibbula umbilicalis*	*Gibbula* spp	*Ensis* spp	*Mytilus edulis*	Crustacea	*Lauria cylindricea*	*Discus rotudatus*	*Aegopinella nitidula*	Spirorbid	Unid
PHASE 3: HISTORIC																		
CCBS:1	*		*	*														
CCBS:2	*		*	*														
CCBS:3	*		*	*														*
PHASE 2: IRON AGE																		
CCBS:4	*		*	*	*							*	*					
CCBS:5	*		*	*	*				*	*		*	*					*
CCBS:6	*		*	*	*					*			*	*			*	
CCBS:7	*		*	*	*	*				*			*				*	*
CCBS:8	*		*	*	*					*	*	*	*			*		
CCBS:9	*	*	*	*	*			*		*	*	*	*		*	*		*
CCBS:10	*		*	*	*		*			*	*	*	*			*		
PHASE 3: BRONZE AGE																		
CCBS:11	*		*	*	*								*					*
CCBS:12	*	*	*	*									*				*	
CCBS:13	*		*	*						*			*					
CCBS:14	*		*	*							*		*					
CCBS:15	*		*	*									*					
CCBS:16	*		*	*									*					

the sequence, it would appear unlikely that either periwinkles or limpets were being over-exploited throughout the period of activity in Croig Cave. In light of the relative large size of the limpets, it would appear that throughout the period of activity at Croig Cave these were collected at the high shore line where the larger shells are found (Cabral and Silva 2003).

Table 20 provides the percentages of complete shells to fragmented shells (in weight percentage) for limpets and periwinkles. The majority of the samples have a higher percentage of fragmented limpets to whole limpets, especially in CCBS:5 and CCBS:12. There is a different trend for periwinkles: 12 out of the 16 samples contain a higher percentage of complete than fragmented periwinkles. The only sample without any complete shells is CCBS:12. Shells differentially preserve and fracture based on variation in their structure, composition and size (Giovas 2009). The frequency of crushed shells within the samples appears insufficient to argue that the shellfish were being used as fishing bait (cf Deith 1989) rather than being collected for human consumption. The relatively high frequency of crushed shell in some of the lower samples is likely to derive from trampling in the cave.

WOOD CHARCOAL

Phil Austin

A total of 1,107 fragments were examined from the 16 samples, resulting in the identification of 15 taxa. 106 fragments could not be identified. These along with bark and hazelnut shell fragments were included in the indeterminate (Indet) category. Table 21 presents the full results of the analysis for each context and sample, with illus 14c showing the quantity of charcoal by sample.

Taxon differentiation

The 15 taxa identified consist of 11 indigenous hardwoods (angiosperms) and four softwoods (gymnosperms). Two of the four softwoods identified, Scots pine (*Pinus sylvestris*) and yew (*Taxus baccata*), are native to Scotland; the two others, larch (*Larix decidua*) and spruce (*Picea abies*) were not native to the British Isles in the Holocene. Larch and spruce are anatomically similar and can be difficult to differentiate. Whilst it is certain that both taxa are represented, it is possible that some of the smaller fragments were incorrectly attributed. This is only of relevance in terms of fragment numbers for each of these taxa and does not affect the fact that both are represented. Willow (*Salix* spp) and poplar (*Populus* sp) are also anatomically very similar and consequentially difficult to differentiate. Heterogeneous rays were, however, observed in the majority of fragments examined, suggesting that most were willow rather than poplar. The two native species of oak (*Quercus petraea* and *Q. robur*) cannot be differentiated anatomically. The present day distribution of the two oaks favours the sessile oak (*Q. petraea*) as the species represented rather than the pendunculate (*Q. robur*). The Maloideae, a sub-family of the Rosaceae, includes genera virtually indistinguishable anatomically and, with the exception of probable rowan (*Sorbus* sp) fragments, no attempt to do so was made here. Cherry/fruits (*Prunus* spp) can be differentiated anatomically but, in most instances, this was not possible in this study. Some fragments were tentatively identified as bird cherry (*Prunus avium*).

Fragment condition and wood form

Overall, the majority of the charcoal recovered was well preserved. Thermal degradation and the accumulation of mineral deposits were not so extreme as to prevent identification or affect the structural integrity of individual fragments. The degree of thermal degradation exhibited was occasionally high, especially in those fragments apparently derived from twigs or small branches, but none of the fragments appeared 'vitrified', the most extreme form of

TABLE 20
Summary statistics of molluscs

	Total weight of fragments & whole shell	*Percentage weight of shell of bulk sample*	*No of species present*	*Percentage shell weight of limpet of total shell weight*	*Percentage shell weight of periwinkle total shell weight*	*Fragmentation: percentage of complete limpet within total weight of limpet*	*Fragmentation: percentage of complete periwinkle within total weight of periwinkle*
PHASE 3: HISTORIC							
CCBS:1	215.20	5.60	3	88.38	10.97	3.21	33.05
CCBS:2	77.77	3.43	3	64.16	33.26	0.00	53.23
CCBS:3	318.61	4.49	4	81.35	17.67	48.69	94.67
PHASE 2: IRON AGE							
CCBS:4	662.47	12.97	6	65.06	33.57	42.99	94.29
CCBS:5	1563.57	34.75	9	24.93	73.79	27.24	49.42
CCBS:6	2222.16	62.85	8	91.23	8.19	54.23	70.45
CCBS:7	1950.04	46.04	9	71.34	27.31	39.41	79.35
CCBS:8	1653.31	34.76	9	59.14	37.86	37.74	68.43
CCBS:9	1355.27	25.01	13	53.83	42.08	40.71	71.61
CCBS:10	1000.08	14.85	10	45.07	50.87	39.36	64.44
PHASE 1: BRONZE AGE							
CCBS:11	688.10	14.44	6	42.61	53.74	37.21	47.81
CCBS:12	141.40	2.33	6	76.03	3.75	20.28	0.00
CCBS:13	79.90	1.06	5	50.06	11.76	34.50	77.66
CCBS:14	203.90	3.08	4	67.24	19.81	53.98	76.98
CCBS:15	114.70	1.86	4	33.13	39.41	38.68	85.62
CCBS:16	90.60	1.69	4	39.62	15.56	46.52	64.54

TABLE 21
Wood charcoal: taxa and quantification

	Taxa	*Qty.*	*Wt.(g)*
	PHASE 3: HISTORIC		
CCBS:1	*Betula* sp	3	0.031
	Calluna vulgaris	11	0.138
	Corylus avellana	32	0.757
	Maloideae (*Sorbus* type)	4	0.430
	Prunus sp	1	0.009
	Pinus sp	2	0.014
	Quercus sp	9	0.214
	Salix/*Populus*	10	0.076
	Taxus baccata	3	0.097
	Indet (inc bark; nutshell)	25	0.678
	Totals: 9 taxa	100	2.444
CCBS:2	*Betula* sp	1	0.031
	Calluna vulgaris	36	0.588
	Corylus avellana	48	0.797
	Fraxinus excelsior	2	0.023
	Prunus sp	1	0.024
	Quercus sp	1	0.013
	Salix sp	1	0.014
	cf *Sambucus nigra*	1	0.025
	Indet (inc bark; nutshell)	8	0.342
	Totals: 8 taxa	100	1.857
CCBS:3	*Betula* sp	6	.134
	Calluna vulgaris	10	0.079
	Corylus avellana	38	0.488
	Fraxinus excelsior	1	0.008
	Prunus sp	4	0.034
	Quercus sp	15	0.197
	Salix/*Populus*	9	0.038
	Taxus baccata	1	0.007
	Indet (inc bark)	16	0.24
	Totals: 8 taxa	100	1.234
	PHASE 2: IRON AGE		
CCBS:4	*Betula* sp	11	0.195
	Calluna vulgaris	6	0.074
	Corylus avellana	52	1.125
	cf Larix decidua	2	0.041
	Maloideae	2	0.046
	Prunus sp *cf P. avium*	2	0.040
	Quercus sp	11	0.245
	Salix/*Populus*	8	0.154
	Indet (inc bark; nutshell)	6	0.095
	Totals: 8 taxa	100	2.015

	Taxa	*Qty.*	*Wt. (g)*
CCBS:5	*Betula* sp	14	0.196
	Calluna vulgaris	2	0.020
	Corylus avellana	57	1.293
	Hedera helix	1	0.021
	Maloideae	1	0.009
	Prunus sp	1	0.014
	Quercus sp	6	0.211
	Salix/Populus	7	0.112
	Indet (inc bark; nutshell)	11	0.160
	Totals: 8 taxa	100	2.036
CCBS:6	*Alnus glutinosa*	5	0.302
	Betula sp	18	0.389
	Corylus avellana	15	0.416
	Picea sp	5	0.098
	Quercus sp	50	2.169
	Salix	3	0.124
	Indet (inc bark; nutshell)	4	0.167
	Totals: 6 taxa	100	3.665
CCBS:7	*Betula* sp	8	0.331
	Corylus avellana	22	0.7
	Picea sp	3	0.119
	Quercus sp	12	0.536
	Salix	38	1.131
	Indet (inc bark)	17	0.722
	Totals: 5 taxa	100	3.539
CCBS:8	*Betula* sp	17	0.438
	Corylus avellana	11	0.276
	Larix sp	2	0.159
	Prunus sp	1	0.015
	Quercus sp	63	2.201
	Salix/Populus	1	0.017
	Indet (inc bark; nutshell)	5	0.293
	Totals: 6 taxa	100	3.399
CCBS:9	*Alnus glutinosa*	1	0.013
	Betula sp	29	0.716
	Corylus avellana	5	0.169
	Hedera helix	1	0.110
	Quercus sp	55	1.489
	Salix sp	2	0.008
	Sorbus sp	1	0.041
	Indet (inc bark)	6	0.330
	Totals: 7 taxa	100	2.876

	Taxa	*Qty.*	*Wt. (g)*
CCBS:10	*Betula* sp	2	0.04
	Corylus avellana	20	0.591
	Quercus sp	27	0.798
	Indet (incl bark)	1	0.103
	Totals: 3 taxa	50	1.492
	PHASE 1: BRONZE AGE		
CCBS:11	*Alnus glutinosa*	2	0.084
	Betula sp	8	0.170
	Corylus avellana	14	0.291
	Quercus sp	15	0.431
	Indet	11	0.298
	Totals: 4 taxa	50	1.274
CCBS:12	*Corylus avellana*	4	0.038
	Quercus sp	8	0.027
	Indet (incl bark)	14	0.118
	Totals: 2 taxa	26	0.183
CCBS:13	*Alnus glutinosa*	3	0.008
	Betula sp	1	0.011
	Calluna vulgaris	1	0.002
	Corylus avellana	2	0.013
	Quercus sp	2	0.01
	Salix sp	3	0.036
	Indet	9	0.043
	Totals: 6 taxa	21	0.123
CCBS:14	*Betula* sp	1	0.016
	Corylus avellana	4	0.034
	Quercus sp	12	0.159
	Indet (incl bark)	8	0.032
	Totals: 3 taxa	25	0.241
CCBS:15	*Alnus glutinosa*	1	0.016
	Corylus avellana	1	0.006
	cf *Pinus* sp	1	0.007
	Quercus sp	4	0.072
	Indet	7	0.117
	Totals: 4 taxa	14	0.218
CCBS:16	*Betula* sp	1	0.003
	Corylus avellana	3	0.019
	Quercus sp	6	0.021
	Indet (incl nutshell)	11	0.193
	Totals: 3 taxa	21	0.236

thermal degradation. Fungal mycelium, varying in abundance from the occasional strand to moderately high concentrations, was observed in fragments from every sample and was not confined to any particular taxa. Invertebrate damage, in the form of galleries or bore-holes, was not noted in any of the fragments examined.

Growth ring characteristics, particularly curvature, the presence of the outermost wood, pith/innermost wood and tyloses (in oak fragments) indicate that the charcoal derived from a mix of stem/branch wood, small branches and twigs. The possible stem-wood and branch wood included examples of wood that were mature and slow grown (narrow rings and, in some instances, heartwood) and fast grown, relatively young wood (wide rings, no discernible heartwood). Bark fragments were present in many samples, suggesting that much of the wood was collected with the bark intact, that is, as unmodified roundwood. No root wood was identified. Many of the indeterminate fragments were derived from wood exhibiting atypical anatomy, recorded here as 'knot-wood', comparable to, for example, the distorted grain of wood that forms around branch junctions.

Taxon representation and relative abundance

A moderately broad range of tree, shrub, climber and sub-shrub taxa were identified, including two non-native coniferous trees. Only oak and hazel (*Corylus avellana*) are represented in every sample and thus are present throughout the entire period of midden formation. Birch (*Betula* spp) and willow/poplar are almost as well represented, each being present in 14 and 10 of the 16 samples, respectively. Heather (*Calluna vulgaris*) and cherry, both represented in six samples, are the next most ubiquitous taxa, followed by alder (*Alnus glutinosa*; five samples) and the Maloideae (four samples). Ash (*Fraxinus excelsior*), ivy (*Hedera helix*), larch, spruce, pine and yew were all present in two samples each, whilst elder (*Sambucus nigra*) was present in a single sample only.

Taxon abundance measured by fragment count and weight reveals that oak, hazel and birch are the three most common woods represented, as they are in terms of ubiquity. Hazel is the most abundant measured by total number of fragments whilst oak is the most abundant by weight. Birch is the third most abundant by both fragment count and weight. Willow/poplar and heather are the next most abundant taxa by fragment count and weight. Unlike oak, hazel and birch, which are present throughout the midden, willow/poplar and heather only become abundant in samples from later contexts. The apparent increased presence of these two taxa, along with the earliest appearance of ash, ivy, larch, Maloideae, spruce, cherry, elder and yew, is evident from CCBS:9 onwards. Samples CCBS:1 to CCBS:9 were large samples (typically >150 fragments) and contained a mean average of seven taxa, whilst CCBS:10 to CCBS:16 were significantly smaller (mostly <30 fragments) and contained a mean average of four taxa. Unlike the fish species and mollusc taxa, there is no evident correlation between the number of taxa and sample size as measured by weight of wood charcoal (illus 15c).

There appears to be a subtle change in taxon representation from CCBS:5 onwards. Samples CCBS:1 to CCBS:5 contain eight or nine taxa per sample, whilst the mean average for the remaining samples (CCBS:6 to CCBS:16) is four taxa only. The quantity of heather recorded increases significantly from CCBS:5 onwards (accounting for 65 of the 66 fragments identified), as does cherry (eight of the 10 fragments identified) and Maloideae (seven of the eight fragments identified). Ash, elder and yew are recorded for the first time, albeit in low quantities. Alder is absent from CCBS:1 to CCBS:5 and is last recorded in CCBS:6. Spruce is also absent from CCBS:1 to CCBS:5. However, unlike alder (represented in a total of five samples below CCBS:6), it is represented in only two samples (CCBS:6 and CCBS:7) and, as an alien species, its occurrence is entirely fortuitous.

Discussion

The woods represented in this charcoal assemblage almost certainly represent discarded fire debris and reflect the use of branch wood for fuel and small branches and twigs for kindling. It is possible that some of the wood may have derived from artefacts disposed of in fire but it is impossible to know if this was so. It is most likely that the remains reflect simple hearths used for everyday activities – for the provision of heat and light and for food processing and protection. Use of the fires within the cave for ritual activities cannot be entirely discounted.

The relative lack of diversity in the lowermost samples (CCBS:10 to CCBS:16) suggests that oak, hazel, birch and alder were readily available and seemingly favoured fuel woods. These taxa are all highly regarded as fuel woods. Willow/poplar (three fragments in CCBS:13), heather (one fragment in CCBS:13) and pine (one fragment in CCBS:15) were the only other taxa identified in CCBS:10 to CCBS:16. This contrasts with later deposits (CCBS:1 to CCBS:9) in which the range of woods used becomes increasingly diverse. Though oak, hazel and birch remain the main woods used, the presence of willow/poplar and heather increases significantly whilst alder declines entirely, being absent in CCBS:1 to CCBS:5. Maloideae and cherry also appear, alongside woods not highly regarded for their fuel value, notably elder and ivy. Heather is also a poor fuel wood, but burns brightly and would have been used as kindling. The ivy fragments may have been attached to a preferred wood such as oak and therefore incidentally charred. The opportunistic use of driftwood from the coastal zone, represented here by larch and spruce, is also evident.

It seems that the increase in the range of woods collected for fuel represents a change in collecting behaviour – from a strategy that had been selective to one more opportunistic in character. Although social and cultural factors may have had an influence upon collecting behaviour on the Isle of Mull, a decline in the availability of preferred fuel woods, like oak, hazel, birch and alder, is considered the principal reason that compelled the population to broaden the range of woods used for fuel.

The low quantity of charcoal recovered from the earliest samples, compared to the considerably large sample size of later deposits, is unlikely to result from taphonomic processes, but indicates greater volumes of wood were being consumed as time progressed. Evidence indicative of fungal attack in fragments from all samples suggests that much of the wood was collected as deadwood from the woodland floor rather than as 'green' wood, such as that made available through clearance or the removal of branches during management procedures. However, the stockpiling of wood for future use cannot be discounted and fungal degradation could have occurred during storage.

OVERVIEW

Croig Cave adds to our growing appreciation of the role of caves in the later prehistoric and historic settlement patterns of western Scotland (Ritchie 1966; Tolan-Smith 2001; Birch & Wildgoose 2004, 2005, 2006; Wildgoose & Birch 2007). Any interpretation of Croig Cave's archaeology is constrained by the small volume of its deposits that have been excavated and subjected to sedimentary and midden analysis. We assume this explains the complete absence of pottery and other artefacts material, except for the amber bead, bracelet and piece of iron slag. Milner and Woodman (2007) have also noted how later prehistoric and historic middens in Ireland have failed to provide any diagnostic artefacts.

The original dimensions of the shelter provided by Croig Cave are difficult to estimate in light of the substantial collapse in front of the current entrance. We suspect that the excavated area was once located in a centre of the cave, although this may itself have varied during the

three millennia during which activity occurred. The most striking character of this activity is the degree of consistency: the processing of shellfish, catching of a diverse range of small fish from low-risk, inshore fishing and the making of small hearths within the cave. There are, however, changes in the composition of the midden through the sequence which may reflect subtle changes in subsistence and other forms of activity.

PHASE 1

The earliest documented activity within the cave dates to *c* 1720–1460 cal BC. This began a phase of Bronze Age activity that lasted for up to 1,000 years, with a minimum of three activity events. Sediment accumulated within the cave from a mix of weathering of the basalt roof and walls of the cave and the deposition of midden material, the latter making a relatively small contribution when compared with later periods of activity. While one must attempt to account for relatively poor preservation in the earliest deposits, the low levels of magnetic susceptibility supports the scarcity of charcoal – to indicate that hearths had been small, infrequent and low intensity. The deposition of mollusc shells was also relatively low in both frequency and species diversity. Fish bones were, however, substantial in number, with a wide range of species being processed, especially towards the end of this phase of activity.

The accumulation of midden deposits within caves during the Bronze Age is known from several sites, including Tinkler's Cave at Lochgilphead (Tolan-Smith 2001), Uamh an ard Achadh (High Pasture Cave), Isle of Skye (Birch & Wildgoose 2004) and Sculptor's Cave, Covesea, Moray (Shepherd 2007; Armit et al 2011). The fish remains within the latter were also diverse with regard to species and noted as coming from especially small fish. Bronze Age middens are also known from open sites in western Scotland, notably at Kilellan, Islay (Ritchie 2005), Northton, Harris (Simpson 1976), and Rosinish, Benbecula (Shepherd & Tuckwell 1977). Quite what contribution fishing and shellfish gathering made to the Bronze Age economy remains unknown; one must assume that this was limited when compared to that of animals and plants, both domesticated and wild.

There appears to have been a significant, although short-lived, change of activity within the cave at *c* 950 cal BC. At least two small shallow pits were dug into the floor, although these appear to have been little more than scoops or even the minor enlargement of natural depressions. A copper bracelet, made with ore originating in Ireland, and a single amber bead were deposited within one of these pits, presumably as a votive offering. The date of *c* 950 cal BC provides a good fit with the typology of the bracelet, which places it within the Ewart Park phase dated to *c* 1020–800 cal BC (Needham et al 1997). The deposition of fine metalwork within caves is well known from the Bronze Age, this often being associated with human remains (Shepherd 2007). The absence of human remains at Croig Cave may simply reflect the limited extent of excavation. The association of a bracelet and amber bead is notable, this also being known from the Glentanar and Balmashanner hoards and the Heathery Burn cave (Pearce 1976). Pearce (1976) suggests that amber was especially important in the Irish Bronze Age, it being transported or traded across northern Britain. In this regard, the Irish origin of the copper ore used to manufacture the bracelet is of particular interest.

PHASE 2

While the available radiocarbon dates suggest a hiatus of activity until *c* 480–200 cal BC and a minimum number of two events during the next *c* 300 years, we suspect that this is primarily a function of the sampling strategy and the low number of dates. Activity is more likely to have been a regular sequence of small

events resulting in the accumulation of midden deposits. The intensity of human activity was variable: on some occasions this was limited, providing the opportunity for weathered basalt and lenses of blown sand to accumulate on the midden surface; at other times, there was a rapid accumulation of midden deposits. Other than towards the end of this Phase, there appears to have been a relative shift from fishing to shellfish collecting, with shells from the latter becoming particularly dense and representing a wide range of species. This might, of course, represent changes in deposition patterns within the cave rather than activity, with fish bones having been concentrated in unexcavated areas.

Midden deposits are commonplace on Iron Age sites of Scotland. They are often found at wheelhouses and brochs (Wickham-Jones 2007), as well as forming extensive deposits, such as at Pool, Orkney (Hunter 1990), and in the Forth Valley (Sloan 1984). Their contribution to the diet as a whole was probably limited; cattle and pig bones make their first appearance in the Croig Cave deposits in this phase of activity.

The number/size of hearths also appears to increase over those of the Bronze Age Phase in light of the substantial increases in charcoal. The piece of iron slag suggests that this might reflect iron smelting and/or smithing within the cave, as is known to have occurred within Keil Cave, Kintyre (Ritchie 1966), and Uamh an ard Achadh, Skye (Birch & Wildgoose 2005).

PHASE 3

The Historic Activity within the cave might derive from one single event at *c* AD 1210, but we again suspect a more continuous sequence of small scale activity events into post-medieval period. Excavated midden deposits from the Pictish, Viking, Norse and later periods are widespread in Scotland, such as at Buckquoy (Ritchie 1977) and Quoygrew (Barrett & Gerrard 2004), both on Orkney. At Croig Cave, the analysis indicates that fishing became dominant over shellfish collecting, but this may again be a reflection of sampling a spatially variable midden deposit. The increase in heather and loss of alder is likely to derive from changes in woodland composition, which will be further explored by comparison with pollen sequences from Mull. The uppermost sample reflects the most intensive fish processing of the whole sequence and has notably high levels of zinc that might derive from the processing of seaweed, potentially for potash. If that was the case, however, one might have expected higher levels of charcoal within the deposits, but these show a significant decline from those within the Phase 2 activity.

SUMMARY

Although a large number of standing monuments for the Bronze and Iron Ages on the Isle of Mull have been documented (RCAHMS 1980), our knowledge of the later prehistoric economy remains limited. Croig Cave provides insights into one element of this economy, showing the collection of limpets and periwinkles, along with a range of other shellfish, and the catching of a diverse range of predominately small fish. It seems likely that this represents a substantial component of the economy, and its most striking characteristic is its continuity for over three millennia while there were, no doubt, significant changes in the wider economy and society. These are indicated within the cave by the Bronze Age deposition of the bracelet and bead, suggesting links with Ireland, and the presence of iron slag indicating smithing or smelting in the cave. Full interpretation of these finds will only be possible from a more extensive excavation within Croig Cave.

ACKNOWLEDGEMENTS

We are grateful to Ian Spence of Penmore, Isle of Mull, for drawing our attention to Croig Cave and to Jill Galbraith of Croig, Isle of Mull, for providing permission to excavate. Technical support for the

midden analysis was provided by Mike Andrews within the School of Human & Environmental Sciences, University of Reading. We are grateful to Lucy Martin for preparing the map and diagrams, and to Marion O'Neil for the drawing of the bracelet and bead. Financial support was kindly provided by the University of Reading.

APPENDIX 1: METHODS

RADIOCARBON DATING AND BAYESIAN MODELLING

Shell samples received an acid etch chemical pre-treatment prior to radiocarbon dating, while the sample of wood underwent acid-alkali-acid washing. Calibration of their conventional radiocarbon ages (^{14}C years BP) was achieved using the probability method in OxCal v4.1.7 (Bronk Ramsey 2009) and the most recent IntCal 09 and Marine09 radiocarbon calibration curves (Reimer et al 2009). Radiocarbon dates obtained from limpet shells were corrected for the local marine reservoir effect (–64 ± 46 years) (Reimer & Reimer 2001). Calibrated date ranges are expressed as cal BC in the 95.4% probability range with their end points rounded up to the nearest 10 years.

Bayesian modelling of radiocarbon dates is becoming widely applied to the evaluation of chronologies within archaeology (eg Buck et al 1994; Blackwell & Buck 2003; Blockley et al 2004; Bayliss et al 2007). This approach incorporates stratigraphic and successional information into the calibration process (Buck et al 1991, 1992) to generate a set of prior (unconstrained) and posterior (constrained) probability distributions for the radiocarbon age determinations. The degree of overlap between the prior and the posterior probability distributions of an individual date is expressed as an agreement index with strongly overlapping distributions giving high values. An agreement index of ≥60% has been recommended as a threshold below which individual dates within a chronological model and for a model as a whole should be rejected (Bronk Ramsey 2008).

The Bayesian probability device incorporated in the OxCal ^{14}C calibration program (Bronk Ramsey 2009) was, therefore, used to calibrate the radiocarbon time-scales for the shell midden. This provided the means by which age-depth inversions could be resolved by constructing a chronological model that initially included all radiocarbon dates in stratigraphic order. Further refinements were then made by eliminating inconsistent dates from the model until a high level of agreement between the dates and the model was attained. Values falling below the agreement index threshold were taken to represent posterior probability distributions that diverged widely from the area of maximum probability of the prior distribution in order to fit within the stratigraphic constraints and, on this basis, were rejected from the Croig Cave chronological model. In the present case, we removed five samples (35% of the total input) reaching an agreement index for the overall model of 100.2%.

Our analysis of the radiocarbon chronology included the use of boundaries to define the beginnings and endings of phases of deposition. Sections of the midden were divided into phases of use according to the alignment of groups of radiocarbon determinations and the separation in time between them. This ensured that the tendency for the generic sequence algorithm used in OxCal to over-estimate the oldest dates within a finite sequence was kept to a minimum (Blockley et al 2004: 161).

Following convention, posterior density estimates are distinguished from calibrated dates by *italics*.

Radiocarbon dates were also subjected to chi-square tests to ascertain evidence of inconsistency (Ward & Wilson 1978); in those cases where there was no such evidence, the dates were deemed to be statistically consistent with the possibility of having derived from a single depositional event. By using chi-square tests it was possible, therefore, to suggest a

minimum number of phases of use of the midden from which the 14 radiocarbon dated samples derived. We use Bayesian modelling procedures cautiously, however, noting Ashmore's (2004) concern that it can add to the complexity of a paper without significantly improving understanding or interpretation.

X-RAY DIFFRACTION (XRD)

Sediment characterisation was achieved by quantifying bulk mineralogy using XRD analysis. Sub-samples of the <2.0–0.5mm and <125μm fraction of each bulk sample were dried and ground in a Tema and Fritch planetary ball mill using agate grinding elements. Powdered sediments were used to fill whole sample mounts using the front-faced riffle-packing method in order to randomly orient samples. The mounts were analysed using a Siemens D500 X-Ray Diffractometer with Diffrac-Plus software, Cu X-ray tube and curved graphite monochromator. Minerals present were identified by reference to known powder diffraction patterns (ICDD Powder Diffraction File Inorganic Subset; Chen 1977) and quantified using a h-factor to calculate whole rock percentage data (Hooton & Giorgetta 1977).

X-RAY FLUORESENCE (XRF)

Individual elements in the powder samples used for XRD analysis were identified and quantified using XRF. This method was used to substantiate the results and interpretation of the XRD data providing a breakdown of the elemental composition of the samples. Compressed powder pellets were analysed to determine major and trace elements. A wide range of international reference standards (Govindaraju 1989) were used to calibrate the instrument and were run in each batch of samples to provide an internal standard check to confirm the quality of the data. Analysis was determined using a Philips PW 1480 X-ray fluorescence spectrometer with a dual anode Sc/Mo 100kV 3kW X-ray tube and X40 analytical software. The nominal detection limit of trace elements was 5ppm, while a standard error at 3 sigma confidence (worst case) of the major elements was a nominal 5%.

PARTICLE SIZE DISTRIBUTION (PSD)

Particle size distributions on the coarse fraction (>500μm) were established by sieve analysis. Bulk samples were processed air-dry through a stack of sieves using sieve apertures set at single phi intervals (64mm, 31.5mm, 16mm, 8mm and 2mm) and placed on a mechanised shaker for 30 minutes. Sample statistics for PSD of both fine and coarse grain sediments are presented as histograms and ternary diagrams (sand/silt/clay) produced using the Gradistat software (Blott & Pye 2001). The application of particle size analysis to archaeological sediments is, however, problematic as the presence of carbonates, iron oxides and organic material can affect results. Interpretations were based, therefore, on mean values and degrees of sorting to allow for comparisons of the different size class inputs to evaluate modes of deposition, that is, mixed anthropogenic inputs versus naturally accreting sediments. Interpretations of skewness were not attempted as these are only meaningful if there is unimodal distribution that allows for standard deviations to be measured, circumstances that we did not expect to encounter in anthropogenic sediments such as these studied here.

LOSS ON IGNITION (LOI)

Loss on ignition of sub-samples of the <2mm sediment fraction was determined using the method of Bascomb (1982) to provide information about the organic content of the midden. About 5g of air-dry sediment was weighed into an ignition resistant container and placed in an oven at 105°C overnight. Water content percentage was calculated using the following formula:

= 100 × [(weight of bulk sample – weight of oven-dried sample)/weight of bulk sample]

The container and contents were re-weighed and placed in a furnace at 950°C for two hours. Samples were placed in a desiccator to cool and re-weighed. Loss on ignition percentage was calculated using the following formula:

= 100 × [(weight of oven-dry sediment – weight of ignited sediment)/weight of oven-dried sediment]

MAGNETIC SUSCEPTIBILITY

Magnetic susceptibility measurements of sub-samples of the <2mm fraction were determined to provide information about pedogenic processes and burning history. Approximately 10g of sediment were placed inside a Bartington Instruments MS2B Dual Frequency Sensor, coupled to a MS2 magnetic susceptibility meter to record low-frequency measurements. Low frequency mass specific magnetic susceptibility (ie bulk magnetic susceptibility/weight) measurements were obtained using The International System of Units (10^{-8} SI/kg).

LEAD ISOTOPE COMPOSITION OF BRACELET AND SLAG

Because the isotopes of Pb are not affected to a measurable extent by physical and chemical processes, they form an ideal environmental tracer, providing an opportunity to locate the source of Pb ore used in the manufacture of artefacts. As three (^{206}Pb, ^{207}Pb and ^{208}Pb) of the four naturally occurring Pb isotopes (^{204}Pb, ^{206}Pb, ^{207}Pb and ^{208}Pb) are end members of radioactive decay chains (^{208}Pb [^{232}Th], ^{207}Pb [^{235}U] and ^{206}Pb [^{238}U]), different ores will have different isotopic composition according to their age and initial U and Th content of the rocks. The isotopic composition of produced Pb oxides, Pb halides and organolead compounds emitted from the burning and production of Pb compounds and metals reflects the Pb isotopic composition of the ore used in production. There are issues relating to the mixing of materials which hamper some interpretations of isotopic data. For example, an artefact produced from one ore locality might be broken and then recast with artefact fragments coming from other ore fields to make a new object with an isotopic composition relating to an ore source from which none of the original fragments had derived. For further discussion of the principles and methods of Pb isotopic analysis and a series of applications, see LeHuray et al (1987); Dixon et al (1990); Arribas et al (1991); Stos-Gale et al (1995); Haggerty et al (1996); Rohl (1996) and Rohl & Needham (1998).

Small samples (15–55mg) of fine metal fragments were removed from the bracelet with a dentist drill (2,000rpm) using small (1mm diameter) acid-washed, stainless steel, diamond-coated drill bits. These were then homogenised in an agate mortar to a fine fraction and dried in an oven at 105°C for 24 hours to remove surface moisture. Further small samples (26–113mg) of corrosion products were removed from the surface of the bracelet. These samples were destructively analysed for lead (Pb) isotopes using a Perkin Elmer ELAN 6000 Inductively Coupled Plasma Mass Spectrometer. Although the mass ratio of the 204/208 isotopes is low (<3%), the counts were increased by running the mass spectrometer in isotope ratio mode using ten replicate analyses, an increased dwell time (100ms) together with an average of 45 passes per replicate sample. This brought the uncertainty of the ratios to within a tolerable level (<1.8%). All aliquots were spiked with internal standards (Re and Rh) in a $10.00 \pm 0.01 \mu$g/L concentration. Detection limits at masses 204 and 208 were better than 6ng after correcting for dead time, background and mass bias. Replication of multiple digestions from single samples was better than 0.6%, whereas replicate aliquot analyses (n = 20) of individual samples was better than 0.3%.

The sample solutions used in the Pb isotopic analysis were also used to determine total metal concentration. These samples were analysed for

a range of metals using the same Perkin Elmer ELAN 6000 Inductively Coupled Plasma Mass Spectrometer.

FISH, ANIMAL AND BIRD BONE

Bone was meticulously recovered from the Croig cave bulk samples using 4mm, 2mm and 1mm sieves providing a representative sample of the types of fish and other animals contained within the deposit. Fifty percent of each sample was examined and recorded using a low power (× 10 magnification) binocular microscope and by reference to comparative material belonging to University of Southampton, Ingrem's personal fish bone collection and identification manuals (Conroy et al 1993; Watt et al 1997). All fragments were recorded to species/family and anatomical element where possible (with the exception of ribs and fin spines) to produce a basic fragment count of the Number of Identified Specimens (NISP).

The proportion of an element represented by each fragment was recorded as < 25%, 25–50%, 50–75% and > 75% according to completeness. Whenever possible, elements were sided. The state of preservation was recorded as good, medium and poor. Few cranial or appendicular elements were present and few were sufficiently complete to allow measurements to be taken. As a consequence, size was visually categorised with the aid of reference specimens following the categories used by Cerón-Carrasco (1999) as follows: very small (< 150mm), small (150–300mm), medium (300–600mm) and large (600–1200mm).

Wrasse was identified to species using jaw and pharyngeal bones, most of the identified remains belong to corkwing (*Crenilabrus melops*). It is probable that most of the bones categorised as Labridae are also corkwing and therefore, when analysing body part representation, all wrasse bones have been combined. This was not possible for species of cod (*Gadus* spp) and hake (*Merluccius* spp) as numerous species are represented. Due to the difficulty of obtaining comparative material and a general scarcity of published illustrations, butterfish (*Pholis gunnellus*) could only be identified using the vertebrae and premaxilla. As a result, body part representation is likely to be biased, particularly in respect of the under-representation of cranial bones.

MOLLUSCS

Mollusc shell was handpicked from each of the sieved bulk samples fractions from the 4mm, 2mm and 1mm meshes. The shell was washed and weighed. Because 85% of identifiable molluscan taxa occur in sieve sizes >6mm (Giovas 2009), the mollusc analysis only considered the remains recovered from the 4mm mesh. The molluscs from the > 4mm fraction were identified using the University of Reading reference collection, with identifications con-firmed by Professor Martin Bell. Fragmented and complete shells were separated for the three main species, *Patella vulgata*, *Littorina littorea* and *Littorina saxatalis* group. Note that for the purposes of this study, all species of *Patella* were categorised as *Patella vulgata*. Complete shells were counted for these three species and morphometric analyses undertaken involving the measurement of height and length/diameter. Absolute weight measurements were also recorded for all species.

WOOD CHARCOAL

Prior to analysis, the samples were wet sieved through 4mm, 2mm, 1mm and 500μm sieves and oven dried at 40°C. Following a sub-sampling strategy recommended by Keepax (1998); but see also Asouti & Austin (2005); Austin (2009), to recover the full range of taxa present in each context, and to aid assessment of taxon abundance, 100 fragments from each sample containing > 100 fragments were randomly selected for detailed analysis. Where samples contained 25–100 fragments, 50

fragments were randomly selected for analysis. Every fragment was examined where samples consisted of <25 fragments. Fragments that could not be identified are recorded as 'indeterminate'. In most instances, *c* 80% of the fragments examined were selected from the >4mm size category and 20% from the 4–2mm category. Below 2mm fragments were too small to enable identification.

Preparation and analysis of the charcoal fragments followed standard procedures, as described in Hather (2000). Identification was aided through reference to the relevant literature, specifically Schweingruber (1990) and Greguss (1954).

Fragments of each taxon identified in each sample were counted during analysis and subsequently weighed as a means of evaluating each taxon's abundance in individual samples, contexts and the assemblage as a whole. Considered separately, neither fragment count nor weight values are reliable indicators of relative abundance (not least because a small quantity of large fragments can weigh more than, or the same as, a large quantity of small fragments of the same taxon). Considered together, however, fragment count and weight values do provide some indication of taxon abundance. As an alternative measure of relative abundance, taxon 'ubiquity' (Popper 1989) was calculated by ranking taxa according to the number of samples in which they were present, regardless of whether a single or many fragments of each taxon was present.

Qualitative analysis of the remains included recording: growth ring counts, ring curvature and widths, along with the presence/absence of pith, innermost wood, outermost wood or bark. Features indicative of relative maturity, such as tyloses in vessels, were also recorded. These observations were made to: (a) assess the comparative maturity of the woods used, that is, twig, branch or stem and if derived from sapwood or heartwood; and (b) to assess growing conditions as reflected in seasonal growth rate, for example, slow or rapid growth (indicated by narrow or wide ring width respectively).

Possible biological degradation, as indicated by the presence of fungal mycelium in vessels and insect galleries/bore-holes, was recorded if present. The intensity of thermal degradation was assessed according to the level of detailed anatomical features retained and the severity of any distortion (radial/tangential splitting). These observations were made to better understand the condition of the wood when collected and burned and the possible character of the fire event(s) in which charring occurred. Nomenclature follows Stace (1997).

REFERENCES

Anderson, A J 1981 'A model of prehistoric collecting on the rocky shore', *Journal of Archaeological Science* 8: 109–20.

Andrew, C J, Crowe, R W A, Finlay, S, Pennell, W M, Pyne S F (eds) 1986 *Geology and Genesis of Mineral Deposits in Ireland*. Dublin: Irish Association for Economic Geology.

Anon 1905 'Notes of the Month', *The Antiquary* 41: 82.

Arribas, A, Tosdal, R M & Wooden, J L 1991 'Lead isotope constraints on the origin of base- and precocious-metal deposits from south-eastern Spain', *in* Pagel, M & Leroy, J L (eds) *Source, Transport and Deposition of Metals* 241–4. Rotterdam: Balkema.

Armit, I, Schulting, R, Knusel, C J & Shepherd, I A G 2011 'Death, Decapitation and Display? The Bronze and Iron Age Human remains from the Sculptor's Cave, Covesea, North-east Scotland', *Proceedings of the Prehistoric Society* 77: 251–78.

Ashmore, P 2004 'Dating forager communities in Scotland', *in* Saville, A (ed) *Mesolithic Scotland and Its Neighbours*, 83–94. Edinburgh: Society of Antiquaries of Scotland.

Asouti, E & Austin, P 2005 'Reconstructing woodland vegetation and its exploitation by past societies, based on the analysis and interpretation of wood charcoal macro-remains', *Environmental Archaeology* 10: 1–18.

Austin, P 2009 'The wood charcoal macro-remains from Mesolithic midden deposits at Sand, Applecross', *in* Hardy, K & Wickham-Jones, C (eds) *Mesolithic and later sites around the Inner Sound, Scotland: the work of the Scotland's First Settlers project 1998–2004*. Scottish Archaeological Internet Reports 31.

Bain, D C, Ritchie, P F S, Clark, D R & Duthie, D M L 1980 'Geochemistry and mineralogy of weathered basalt from Morvern, Scotland', *Mineralogical Magazine* 43: 865–72.

Barrett J & Gerrard J 2004 'Quoygrew-Nether Trenabie', *Discovery and Excavation Scotland* 5: 97–8.

Bascomb, C L 1982 'Physical and chemical analysis of <2 mm samples: water content and loss-on-ignition', *in* Avery, B W & Bascomb, C L (eds) *Soil Survey Technical Monograph No 6: Soil Survey Laboratory Methods*, 14–41. Cranfield: Harpenden.

Bateman, N & Locker, A 1982 'The sauce of the Thames', *The London Archaeologist* 4(8): 204–7.

Bayliss, A, Bronk Ramsey, C, Van Der Plicht, J & Whittle, A 2007 'Bradshaw and Bayes: towards a timetable for the Neolithic', *Cambridge Archaeological Journal* 17: 1–28.

Beck, C & Shennan, S 1991 *Amber in Prehistoric Britain*. Oxford: Oxbow Books.

Benton, S 1931 'The excavation of the Sculptor's Cave, Covesea, Morayshire', *Proc Soc Antiq Scot* 65: 177–216.

Beveridge, E 1903 *Coll and Tiree: their prehistoric forts and ecclesiastical antiquities with notices of ancient remains in the Treshnish Isles*. Edinburgh: T & A Constable.

Birch, S & Wildgoose, M 2004 'Uamh an ard Achadh', *Discovery & Excavation Scotland* 5: 80.

Birch, S & Wildgoose, M 2005 'Uamh an ard Achadh', *Discovery & Excavation Scotland* 6: 88–9.

Birch, S & Wildgoose, M 2006 'Uamh an ard Achadh', *Discovery & Excavation Scotland* 7: 102.

Blackwell, P G & Buck, C E 2003 'The Late Glacial human reoccupation of north-western Europe: new approaches to space-time modelling', *Antiquity* 77: 232–40.

Blockley, S P E, Lowe, J J, Walker, M J C, Asioli, A, Trincardi, F, Coope, G R & Donahue, R E 2004 'Bayesian analysis of radiocarbon chronologies: examples from the European Late-glacial', *Journal of Quaternary Science* 19: 159–75.

Blott, S & Pye, K 2001 'Gradistat: a grain size distribution and statistics package for the analysis of unconsolidated sediments', *Earth Surface Processes and Landforms* 26: 1237–48.

Briggs, S 1997 'The discovery and origins of some Bronze Age amber beads from Ballycurrin Demesne, Co Mayo', *Journal of the Galway Archaeological & Historical Society* 49: 104–21.

Britton, D & Longworth, I H 1969. 'Late Bronze Age finds from Heathery Burn cave, County Durham', *British Museum Quarterly* 35: 20–38.

Bronk Ramsey, C 2008 'Deposition models for chronological records', *Quaternary Science Reviews* 27: 42–60.

Bronk Ramsey, C 2009 'Bayesian analysis of radiocarbon dates', *Radiocarbon* 51: 337–60.

Buck, C E, Christen, J A, Kenworthy, J B & Litton, C D 1994 'Estimating the duration of archaeological activity using ^{14}C determinations', *Oxford Journal of Archaeology* 13: 229–40.

Buck, C E, Kenworthy, J B, Litton, C D & Smith, A F M 1991 'Combining archaeological and radiocarbon information: a Bayesian approach to calibration', *Antiquity* 65: 808–21.

Buck, C E, Litton, C D & Smith A F M 1992 'Calibration of radiocarbon results pertaining to related archaeological events', *Journal of Archaeological Science* 19: 497–512.

Burley, E 1956 'A catalogue and survey of the metal-work from Traprain Law', *Proc Soc Antiq Scot* 89: 118–226.

Cabral, J P & Silva, A C F 2003 'Morphometric analyses of limpets from an Iron Age shell midden found in northwest Portugal', *Journal of Archaeological Science* 30: 817–29.

Cahill, M 2006 'John Windele's Golden Legacy – Prehistoric and Later Gold Ornaments from Co. Cork And Co. Waterford', *Proceedings of the Royal Irish Academy* C 106: 219–337.

Cerón-Carrasco, R 1998 'The Fish Remains', *in* Lowe C (ed) *St. Boniface Church, Orkney: Coastal Erosion and Archaeological Assessment*, 149–55. Stroud: Sutton Publishing and Historic Scotland.

Cerón-Carrasco, R 1999 'The fish bones', *in* Parker Pearson, M, Sharples, N, Mulville J & Smith, H (eds) *Between Land and Sea: Excavations at Dun Vulan, Research Vol 3*, 234–74. Sheffield: Sheffield Academic Press.

Cerón-Carrasco, R 2003 'The Fish Remains from Geirisclett Chambered Tomb', *in* Dunwell, A, Johnson, M & Armit I (eds) Excavations at Geirisclett chambered cairn, North Uist, Western Isles, *Proc Soc Antiq Scot* 133: 1–33.

Chanin, P 1988 *Natural History of Otters*. London: Christopher Helm Publishing Ltd.

Chen, P 1977 'Table of key lines in X-ray powder diffraction patterns of minerals in clays and associated rocks', *Department of Natural Resources Geological Survey Occasional Paper 21*.

Classen, C 1998 *Shells*. Cambridge: Cambridge University Press.

Coles, J M 1960 'Scottish Late Bronze Age metalwork: typology, distributions and chronology', *Proc Soc Antiq Scot* 93: 16–134.

Colley, S 1983 *The role of fish bone studies in economic archaeology: with special reference to the Orkney Isles*. Unpublished PhD thesis, University of Southampton.

Conroy, J W H, Watt, J. Webb, J B & Jones, A 1993 *A Guide to the Identification of Prey Remains in Otter Spraints*. London: The Mammal Society.

Cowie, T 2006 'Breachacha House or Breachacha (New) Castle, Isle of Coll', *Discovery & Excavation Scotland* 7: 27.

Cowie, T, O'Connor, B & Proudfoot, E 1991 'A Late Bronze Age hoard from St Andrews, Fife, Scotland: a preliminary report', *in* Chevillot, C. & Coffyn, A (eds) *L'age du bronze atlanqitue: ses faciés, de l'Écosse à l'Andalousie et leurs relations avec le brtonze continental et la méditerranée: Actes du ler Colloque du Parc Archéologique de Beynac*, 49–58. Publication de l'Association des Musées du Sarladais.

Cutting, C L 1956 *Fish Saving*. New York: Philosophical Library.

Deith, M R 1989 'Clams and Salmonberries: Interpreting Seasonality data from shells', *in* Bonsall C (ed) *The Mesolithic in Europe*, 73–9. Edinburgh: John Donald.

Dixon, P R, Le Huray, A P & Rye, D M 1990 'Basement geology and tectonic evolution of Ireland as deduced from Pb isotopes', *Journal of the Geological Society of London* 147: 121–32.

Eogan, G 1967 'The Mull ("South of Ireland") hoard', *Antiquity* 41: 56–7.

Eogan, G 1983 *The Hoards of the Irish Later Bronze Age*. Dublin: University College.

Eogan, G 1994 *The Accomplished Art*. Oxford: Oxbow Books (= Oxbow Monographs 42).

Fenton, A 1978 *The Northern Isles: Orkney and Shetland*. Edinburgh: John Donald.

Giovas, C M 2009 'The shell game: analytical problems in archaeological mollusc quantification', *Journal of Archaeological Science* 36: 1557–64.

Govindaraju, K 1989 'Compilation of working values and sample description for 272 geostandards', *Geostandards Newsletter* 13: 1–113.

Graham, A 1988 *Molluscs: Prosobranch and Pyramidellid Gastropods*. New York: E J Brill/ Dr W Backhuys.

Greguss, P 1954 *The Identification of Central-European Dicotyledonous Trees and Shrubs Based on Xylotomy*. Budapest: The Hungarian Museum of Natural History.

Haggerty, R, Budd, P, Rohl, B & Gale, N H 1996 'Pb-isotopic evidence for the role of Mesozoic basins in the genesis of Mississippi Valley-type mineralization in Somerset, UK', *Journal of the Geological Society of London* 153: 673–76.

Hather, J. 2000 *The Identification of the Northern European Woods. A Guide for Archaeologists and Conservators*. London: Archetype.

Hawkes, C F C & Clarke, R R 1963 'Gahlstorf and Caister-on-Sea: two finds of Late Bronze Age Irish gold', *in* Foster, L & Alcock, L (eds) *Culture and Environment: Essays in Honour of Sir Cyril Fox*, 193–250. London: Routledge & Keegan Paul.

Hooton, D H & Giorgetta, N E 1977 'Quantitative X-ray diffraction analysis by a direct calculation method', *X-Ray Spectrometry* 6: 2–5.

Hunter, J R 1990 'Pool, Sanday, a case study for the Late Iron Age and Viking periods', *in* Armit, I (ed) *Beyond the Brochs*, 175–93. Edinburgh: Edinburgh Press.

Ingrem, C. 2000 'The fish bones', *in* Branigan, K & Foster, P (eds) *From Barra to Berneray: Archaeological Survey and Excavation in the Southern Isles of the Outer Hebrides*, 303–4. Sheffield: Academic Press.

Ingrem, C. 2005 'Fish remains', *in* Sharples, N (ed) *A Norse Farmstead in the Outer Hebrides. Excavations at Mound 3, Bornais, South Uist*, 157. Oxford: Oxbow Books.

Ingrem, C. forthcoming a 'Fish bones', *in* Parker Pearson, M (ed) *Excavations at Cladh Hallan, South Uist*.

Ingrem, C forthcoming b 'Fish bones', *in* Sharples, N (ed) *Excavations at Bornish Mound 1*.

Ingrem, C forthcoming c 'The fish bones', *in* Parker Pearson, M (ed) *Excavations of a Norse settlement at Kilpheder, South Uist*.

Johnstone, J D 1999 'Regional fluid flow and the genesis of Irish Carboniferous base metal deposits', *Mineralium Deposits* 34: 571–98.

Keepax, C 1988 *Charcoal Analysis with Particular Reference to Archaeological Sites in Britain*. Unpublished PhD thesis, University of London.

Le Maitre, R W, Streckeisen, A, Zanettin, B, Le Bas, M J, Bonin, B, Bateman, P, Bellieni, G, Dudek, A, Efremova, S, Keller, J, Lamere, J, Sabine, P. A, Schmid, R, Sorensen, H & Woolley, A R 2002 *Igneous Rocks: A Classification and Glossary of Terms, Recommendations of the International Union of Geological Sciences*. Sub-commission of the Systematics of Igneous Rocks, Cambridge: Cambridge University Press.

Le Huray, A P, Caulfield, J B D, Rye, D M & Dixon, P R 1987 'Basement controls on sediment-hosted Zn-Pb deposits: a Pb isotope study of carboniferous mineralization in central Ireland', *Economic Geology* 82:, 1695–709.

Longley, D 1980 *Runnymede Bridge 1976: Excavations of a site of Late Bronze Age Settlement*. Guildford: Surrey Archaeology Society Research, Volume 6.

Longworth, G & Tite, M S 1977 'Mossbauer and magnetic susceptibility studies of iron oxides in soils from archaeological sites', *Archaeometry* 19: 3–14.

Lunde, G 1970 Analysis of trace elements in seaweed. *Journal of the Science of Food and Agriculture* 21: 416–18.

Lunkad, S K & Raymahashay, B C 1978 'Ground water quality in weathered Deccan Basalt of Malwa Plateau, India', *Quarterly Journal of Engineering Geology and Hydrogeology* 11: 273–7.

Lynch, F 1991 *Prehistoric Anglesey*, 2nd edn. Anglesey: Anglesey Antiquarian Society.

McArthur, J M, Howarth, R J & Bailey, T R 2001 'Strontium isotope stratigraphy: Lowess Version 3: Best fit to the marine Sr-Isotope Curve for 0–509 Ma and accompanying look-up table for deriving numerical age', *Journal of Geology* 109: 155–70.

McGillivray, W 1876–8. 'Notice of a bronze sword (Exhibited by John L. Stewart, Esq. of Coll), and other antiquities, found in that Island', *Proc Soc Antiq Scot* 12: 686.

Mellars, P A & Wilkinson, M R 1980 'Fish otoliths as indicators of seasonality in prehistoric shell middens: the evidence from Oronsay (Inner Hebrides)', *Proceedings of the Prehistoric Society* 46: 19–44.

Milner, N. & Woodman, P. 2007 'Deconstructing the myths of Irish shell middens', *in* Milner, N, Craig, O E & Bailey, G N (eds) *Shell Middens in Atlantic Europe*, 101–10. Oxford: Oxbow Books.

Morand, P, Carpentier, B, Charlier, R H, Mazé, J, Orlandini, M, Plunkett, B A & De Waart, J 1991 'Bioconversion of seaweeds', *in* Guiry, M D and Blunden, G (eds) *Seaweed Resources in Europe*, 95–148. Chichester: John Wiley & Sons Ltd.

Needham, S, Bronk Ramsey, C, Coombs, D, Cartwright, C & Pettit, P 1997 'An independent chronology for British Bronze Age metalwork: the results of the Oxford Radiocarbon Accelerator programme', *Archaeological Journal* 154: 55–107.

Needham, S P & Spence, T 1996 *Refuse and Disposal at Area 16 East, Runnymede, Runnymede Bridge Research Excavations*, *volume 2*. London: British Museum Press.

O'Brien, W 2004 *Ross Island. Mining, Metal and Society in Early Ireland*. National University Galway, Department of Archaeology: Bronze Age Studies, 6.

O'Connor, B 1980 *Cross-Channel relations in the Later Bronze Age* (2 vols). Oxford: British Archaeological Reports International Series 91.

Parker Pearson M, Sharples, N & Symonds, J 2004 *South Uist: Archaeology and History of a Hebridean Island*. Stroud: Tempus Publishing Ltd

Pearce, S 1971 'A late Bronze Age hoard from Glentanar, Aberdeenshire', *Proc Soc Antiq Scot* 103: 57–64.

Pearce, S 1976 'Amber beads from the late Bronze Age hoard from Glentanar, Aberdeenshire', *Proc Soc Antiq Scot* 108: 124–9.

Popper, V S 1989 'Selecting quantitative measurements in palaeoethnobotany', *in* Hastorf, C A & Popper, V S (eds) *Current Palaeoethnobotany*, 53–71. Chicago: University of Chicago Press.

RCAHMS 1980 *The Royal Commission on the Ancient and Historical Monuments of Scotland. Argyll: an inventory of the monuments volume 3: Mull, Tiree, Coll and Northern Argyll (excluding the early medieval and later monuments of Iona),* Edinburgh: RCAHMS.

Reimer, P J, Baillie, M G L, Bard, E, Bayliss, A, Beck, J W, Blackwell, P G, Bronk Ramsey, C, Buck, C E, Burr, G S, Edwards, R L, Friedrich, M, Grootes, P M, Guilderson, T P, Hajdas, I, Heaton, T J, Hogg, A G, Hughen, K A, Kaiser, K F, Kromer, B, McCormac, F G, Manning, S W, Reimer, R W, Richards, D A, Southon, J R, Talamo, S, Turney, C S M, Van Der Plicht, J & Weyhenmeyer, C E 2009 'IntCal09 and Marine09 radiocarbon age calibration curves, 0–50,000 years cal BP', *Radiocarbon* 51: 1111–50.

Reimer, P J & Reimer, R W 2001 'A marine reservoir correction database and on-line interface', *Radiocarbon* 43: 461–3.

Ritchie, A 1977 'Excavation of Pictish and Viking age farmsteads at Buckquoy, Orkney'. *Proc Soc Antiq Scot* 108: 174–227.

Ritche, A 2005 *Kilellan Farm*. Edinburgh: Society of Antiquaries of Scotland.

Ritchie, J N G 1966 'Keil Cave, a late Iron Age cave in Kintyre', *Discovery and Excavation in Scotland* 99: 104–11.

Rohl, B M 1996 'Lead isotope data from the Isotrace Laboratory, Oxford: Archaeometry Data Base 2, Galena from Britain and Ireland', *Archaeometry* 38: 165–80.

Rohl, B M & Needham, S 1998. *The Circulation of Metal in the British Bronze Age: The Application of Lead Isotope Analysis*. London: British Museum Occasional Paper 102.

Schmidt, P K & Burgess, C B 1981 *The Axes of Scotland and Northern England*. Munich: C H Beck.

Schweid, R 2002 *Consider the Eel*. Chapel Hill & London: University of North Carolina Press.

Schweingruber, F H 1990 *Mikroskopische Holzanatomie. Anatomie Microscopique du Bois. Microscopic wood anatomy*. Swiss Federal Institute of Forestry Research.

Shepherd, I A G 2007 'An awesome place. The late Bronze Age use of the Sculptor's Cave, Covesea, Moray', *in* Burgess, C, Topping, P & Lynch, F (eds) *Beyond Stonehenge: Essays on the Bronze Age in Honour of Colin Burgess*, 194–203. Oxford: Oxbow Books.

Shepherd, I A G & Tuckwell, A 1977 'Traces of Beaker period cultivation at Rosinish, Benbecula', *Proc Soc Antiq Scot* 108: 108–13.

Sloan, D 1984 'Shell middens and chronology in Scotland', *Scottish Archaeological Review* 3: 73–9.

Simpson, D D A 1976 'The late Neolithic and Beaker period settlement at Northton, Harris', *in* Burgess, C & Miket, R (eds) *Settlement and Economy in the Second and Third Millennium BC*, 221–32. Oxford: British Archaeological Reports.

Singer, A 1970 'Weathering products of basalt in the Galilee. 1. Rock-soil interface weathering', *Israel Journal of Chemistry* 8: 459–68.

Singer, A 1973 'Weathering products of basalt in the Galilee and Menashe. II. Vesicular and saprolitic weathering', *Israel Journal of Earth Science* 22: 229–42.

Stace, C 1997 *New Flora of the British Isles*, 2nd edn. Cambridge: Cambridge University Press.

Starley, D 2002 'An Introduction to metal working evidence on archaeological sites – preparation and planning', *Historical Metallurgy Society Data Sheet* 16.

Stos-Gale, Z, Gale, N H, Houghton, J & Peakman, R 1995 'Lead isotope data from the Isotrace Laboratory, Oxford: Archaeometry Data Base 1, Ores from the Western Mediterranean', *Archaeometry* 37: 407–15.

Tite, M S 1972 'The influence of geology on the magnetic susceptibility of soils on archaeological sites', *Archaeometry* 14: 229–36.

Tolan-Smith, C 2001 *The Caves of Mid Argyll*. Edinburgh: Society of Antiquaries of Scotland.

Walker, M J C 2005 *Quaternary Dating Methods*. Chichester: John Wiley.

Wang, T, Surge, D, & Mithen, S J 2012 'Seasonal temperature variability of the Neoglacial and Roman Warm Period reconstructed from oxygen isotope ratios of limpet shells (*Patella vulgata*), Northwest Scotland', *Palaeogeography, Palaeo-climatology, Palaeoecology* 317–18: 104–13.

Ward, G K & Wilson, S R 1978 'Procedures for comparing and combining radiocarbon age determinations: a critique', *Archaeometry* 20: 19–31.

Watt, J 1992 *Prey Selection by Coastal Otters*. Unpublished PhD thesis, University of Aberdeen.

Watt, J 1995 'Seasonal and area-related variations in the diet of otters *Lutra lutra* on Mull', *Journal of the Zoological Society of London* 237: 179–94.

Watt, J, Pierce G J, & Boyle, P R 1997 *Guide to the Identification of North Sea Fish Using Premaxilla and Vertebrae*. Copenhagen: International Council for the Exploration of the Sea.

Wheeler, A 1967 *The Fishes of the British Isles and North-West Europe*. London: Macmillan.

Wickham-Jones, C 2007 'Middens in Scottish prehistory: time, space and relativity', *in* Milner, N, Craig, O E & Bailey, G N (eds) *Shell Middens in Atlantic Europe*, 86–93. Oxford: Oxbow Books.

Wildgoose, M & Birch, S 2007 'Uamh an Eich Bhric', *Discovery & Excavation Scotland* 8: 107.